Faculteit Industriële Ingenieurswetenschappen

master in de industriële wetenschappen: chemie

Masterthesis

Encapsulation of hexanal in Calcium based squaric acid metal organic frameworks UTSA-280

Tuur Bollen

Scriptie ingediend tot het behalen van de graad van master in de industriële wetenschappen: chemie

PROMOTOR :
Prof. dr. ir. Mieke BUNTINX

PROMOTOR :
Prof. dr. Ajay KATHURIA

Gezamenlijke opleiding UHasselt en KU Leuven

Universiteit Hasselt | Campus Diepenbeek | Faculteit Industriële Ingenieurswetenschappen | Agoralaan Gebouw H - Gebouw B | BE 3590 Diepenbeek

Universiteit Hasselt | Campus Diepenbeek | Agoralaan Gebouw D | BE 3590 Diepenbeek
Universiteit Hasselt | Campus Hasselt | Martelarenlaan 42 | BE 3500 Hasselt

2023
2024

Faculteit Industriële Ingenieurswetenschappen

master in de industriële wetenschappen: chemie

Masterthesis

Encapsulation of hexanal in Calcium based squaric acid metal organic frameworks UTSA-280

Tuur Bollen

Scriptie ingediend tot het behalen van de graad van master in de industriële wetenschappen: chemie

PROMOTOR :

Prof. dr. ir. Mieke BUNTINX

PROMOTOR :

Prof. dr. Ajay KATHURIA

UHASSELT KU LEUVEN

Preface & acknowledgement

Experimental work was performed at the California Polytechnic State University in the Department of Industrial Technology and Packaging in San Luis Obispo, California, USA. This thesis marks the end of my studies in chemical engineering in packaging and polymers at the University of Hasselt.

First, I would like to thank my California Polytechnic State University supervisor, Prof Dr Ajay Kathuria. Learning so much from such an educated man has been an honor. I am grateful for the opportunity to learn together during my exchange. Thank you for showing me another side of the academic world I had yet to be able to discover and for all the tips you provided me with. I appreciate all your help and learned a lot from you.

I want to thank Prof. Dr. Kivy Mohsen Beyramali for training me on XRD and SEM. In addition, I would like to thank Prof. Dr. Leslie Sachiyo Hamachi for her help with DSC.

Next, I would like to show my appreciation to Prof Dr Ir Mieke Buntinx; without her help obtaining the internship, none of this would have been possible. I never thought an exchange like this was possible until she gave me the opportunity of a lifetime. Her valuable insight, not only in this thesis but also throughout my studies, helped me grow and taught me so much.

I would also like to thank my family, who supported me all my life. My parents always supported me and motivated me to complete this complex study. Without their support, I would not be where I am now. I want to thank my girlfriend, who stuck by me and supported me on this journey.

I also want to thank my roommates and friends I made in San Luis Obispo; they truly made me feel welcome, and I hope to keep in contact in the future. Subsequently, my classmates in Belgium deserve some credit since I enjoyed sharing this journey with them, and I wish them nothing but the best.

Table of content

List of tables

List of figures

List of abbreviations

1-MCP:	1-methylcyclopropene
AC:	Active Carbon
$Ca(OH)_{2:}$	Calcium hydroxide
CD:	Cyclodextrin
CO_2:	Carbon di oxide
DMF:	*N,N*-Dimethylformamide
DSC:	Differential Scanning Calorimetry
EPA:	U.S. Environmental Protection Agency
FTIR:	Fourier Transform Infrared Spectroscopy
GRAS:	generally recognized as safe
IP:	Intelligent Packaging
IUPAC:	International Union of Pure and Applied Chemistry.
MOFs:	Metal organic frameworks
SEM:	scanning electron microscopy
TGA:	Thermogravimetric Analysis
TTIs:	Time Temperature Indicators
VOCs:	Volatile Organic Compounds
XRD:	X-ray Diffraction

Abstract in English

High surface area porous materials have been researched for various applications in the recent years. Metal organic frameworks (MOFs), a vast family of porous compounds are created by combining metal ions with organic linkers to form complex 3D structures. These pores can be engineered to encapsulate active molecular species, and control their release kinetics in the headspace of food packaging for shelf life extension. The aim of this study is to synthesize a calcium squarate acid MOF, also known as UTSA-280, using a mechano-chemical synthesis process, thereby exploring the feasibility and advantages of calcium, substituting transition metals typically employed in MOF synthesis. Hexanal, a volatile antimicrobial compound, was encapsulated in UTSA-280 crystals via a vapor diffusion process. After synthesis, UTSA-280 crystals were characterized before and after hexanal encapsulation using X-ray diffraction (XRD), Fourier transform infrared spectroscopy (FTIR), thermogravimetric analysis (TGA), differential scanning calorimetry (DSC), and scanning electron microscopy (SEM). XRD patterns, FTIR spectra and SEM images indicate that the UTSA-280 crystals were successfully synthesized. FTIR, TGA and DSC analyses conclude that encapsulation was successful, with TGA showing that UTSA-280 can encapsulate approximately ~20 wt% hexanal.

Abstract in Dutch

Verschillende poreuze stoffen zijn de afgelopen jaren onderzocht voor diverse toepassingen. Metal organic frameworks (MOF's) zijn een uitgebreide familie van poreuze materialen, die worden gevormd door metaalionen te combineren met organische linkers om complexe driedimensionale structuren te vormen. De poriën kunnen specifiek worden ontworpen om actieve moleculen in op te slaan, die nadien op gecontroleerde wijze worden vrijgezet om zo bv. de houdbaarheid van voedsel te verlengen. Deze studie beoogt het synthetiseren van een calcium kwadraatzuur MOF, ook bekend als UTSA-280, door middel van een mechanisch-chemisch syntheseproces. Hierbij wordt ook de haalbaarheid van calcium als vervanger van traditionele transitiemetalen in MOF's onderzocht. Hexanal, een vluchtige antimicrobiële verbinding, wordt geïntegreerd in UTSA-280-kristallen via een dampdiffusieproces. Voor en na de hexanal encapsulatie, worden de gesynthetiseerde UTSA-280-kristallen gekarakteriseerd met behulp van X-stralen diffractie (XRD), Fourier transform infrarood spectroscopie (FTIR), thermogravimetrische analyse (TGA), differentiële scanning calorimetrie (DSC) en scanning elektronenmicroscopie (SEM). XRD-patronen, FTIR-spectra en SEM-beelden bewijzen dat de UTSA-280-kristallen succesvol zijn gesynthetiseerd. FTIR-, TGA- en DSC-analyses bevestigen dat de inkapseling succesvol was, waarbij TGA aantoont dat UTSA-280 ongeveer ~20 wt% hexanal kan opslaan.

1 Introduction

1.1 Context

A significant problem humanity is facing, is the loss of 1/3 of post-harvest food, due to a lack of qualitative storage. Therefore, in a collaborative research project with California Polytechnic State University in San Luis Obispo, USA and the university of Hasselt, Belgium, the objective is to research metal organic frameworks (MOFs). MOFs constitute a class of porous supramolecular materials which can encapsulate a range of molecular species including gases, organic vapor, enzymes and ions. They can be tailored in diverse structural configurations. These materials possess high surface area, catalysis, and selective gas separation properties. Additionally, they exhibit extended-release kinetics of encapsulated molecules. The properties listed above find applications across various industries, including food and pharmaceutical packaging. Figure 1 demonstrates that MOFs consist of two main components: metal ions and organic linkers. During synthesis, the linkage between them forms a crystal lattice. After continuous growth, an extended crystal structure is formed. These porous structures have emerged as a potential solution to reduce post-harvest losses by offering porous structures when incorporated into packaging materials. Despite promising characteristics, including high surface area and tunability, there are environmental and stability concerns, such as biocompatibility and cytotoxicity, that limit their widespread adoption. Furthermore, most MOF structures are currently derived from transition metal nodes and petroleum-based building units, posing challenges for mass application. However, researchers are exploring solvent-free mechanochemical synthesis techniques to enhance stability and scalability for broader commercial applications, including active and intelligent packaging in the food sector [1]. Additionally, hexanal, a gas with well-known antifungal and antimicrobial properties will be incorporated in the porous structures of MOFs.

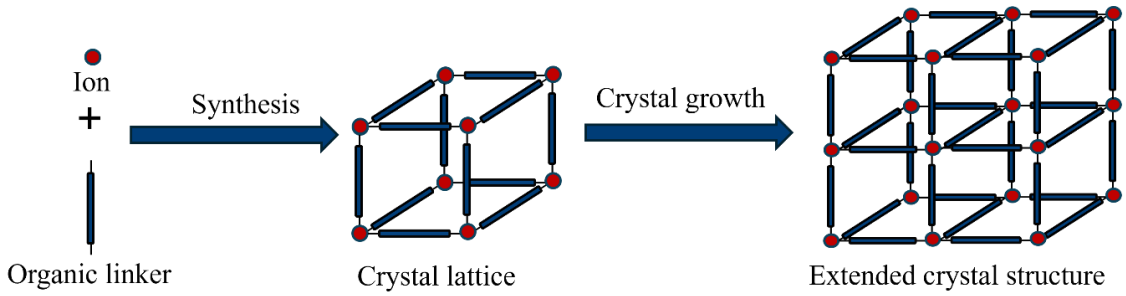

Figure 1: Formation of metal organic frameworks [1]

Calcium metal organic frameworks (Ca-MOFs) are a unique subclass of MOFs known for their stability, low toxicity, and relatively low density. While less extensively researched than transition metal-based MOFs, Ca-MOFs hold promise for applications in molecular separations, electronics, magnetism, and biomedicine. Their advantages include high biocompatibility with drug delivery and efficient adsorption and storage of light molecules due to their gravimetric benefits. Ca-MOFs, characterized by ionic-like solid bonds due to calcium's high electropositivity, have high thermal stability. With calcium being both highly available and non-toxic, Ca-MOFs are cost efficient and environmentally safe, making them ideal for all sorts of applications [2], [3]. Therefore, a novel calcium based sqauric acid MOF will be the focus of this research. Consequently, this research focuses on synthesizing a novel calcium squaric acid MOF (UTSA-280), its characterization and encapsulation of hexanal in UTSA-280 for active packaging application.

1.2 Problem statement/research question

Ca-MOFs hold tremendous potential in various fields, from gas storage to drug delivery. However, a significant problem has hampered their practical utility: the time-consuming synthesis process. Traditional methods often require three days to produce the UTSA-280 MOFs [4]. This prolonged synthesis time hinders large-scale production and slows down research progress and practical applications. To address this issue, researchers are turning to swift synthesis processes of Ca-MOFs. One recently identified method can synthesize Ca-MOFs in only two minutes. In this method, calcium oxide and squaric acid are ground for two minutes to form a grey powder [5]. This breakthrough can potentially revolutionize the field, making Ca-MOFs more accessible and facilitating their integration into various applications. Therefore, in this research, the two-minute mechanochemical synthesis will be further developed to expand the production of Ca-MOFs to an industrial level.

In addition to the long synthesis time, another pressing concern is the short shelf life of many food products, especially fresh produce, leading to significant economic losses and food waste. In response, researchers are exploring innovative strategies to extend shelf life, and one promising avenue involves incorporating hexanal into UTSA-280. Hexanal, a well-known antimicrobial and antifungal compound which delays ripening, presents a suitable solution to enhance food preservation. Researchers aim to create a stable and controlled-release system for this bioactive compound by encapsulating hexanal within Ca-MOFs. This approach not only addresses the issue of short shelf life but also offers a sustainable alternative to traditional preservatives, reducing the reliance on synthetic chemicals and preventing potential health risks associated with their use. Incorporating hexanal into Ca-MOFs holds significant promise for various food products, including fruits, vegetables, and packaged goods. By extending the shelf life of perishable items, this research can enhance food security, reduce waste, and contribute to sustainable food supply chains [6]. The primary challenge lies in effectively encapsulating hexanal for an extended time due to its highly volatile nature [7].

1.3 Research objectives

The primary objective of this research is to validate the synthesis of UTSA-280, a novel MOF, within minutes, a significant improvement over traditional methods that typically takes three days. The synthesis aims to ensure the MOF's biocompatibility and thermal stability by incorporating calcium ions and squaric acid as a bioderived linker. Following synthesis, the second objective is to characterize the crystals using the following techniques: X-ray Diffraction (XRD), Fourier Transform Infrared Spectroscopy (FTIR), Thermogravimetric Analysis (TGA), Differential Scanning Calorimetry (DSC), and scanning electron microscopy (SEM). These analyses aim to determine the properties of crystals synthesized in two minutes.

Moreover, the study seeks to investigate the encapsulation of hexanal within UTSA-280 for potential applications in active food packaging. XRD, FTIR, TGA, DSC, and SEM will also characterize the encapsulation process. In order to improve the shelf-life significantly, stable release kinetics of hexanal are desired. Quantitative analysis determines the amount of hexanal successfully encapsulated within UTSA-280, providing valuable insights into its effectiveness as a carrier for active packaging applications.

2 State of the art

2.1 General introduction

Food waste poses a significant environmental challenge, with over a third of food lost or wasted in the supply chain annually, which leads to significant economic losses. The environmental impact, particularly greenhouse gas emissions and climate change, has gained increased attention from various organizations and agencies worldwide. To address this issue, technological advancements in post-harvest food processing, packaging, and supply chain management offer promising solutions. Active packaging technologies can control physical, chemical, and biological processes leading to food spoilage and waste, mitigating greenhouse gas emissions. These innovations, coupled with consumer education and governmental policies promoting sustainable practices, hold the potential to substantially reduce food waste and create a more efficient and environmentally friendly food system [1].

2.2 Active packaging

2.2.1 Opportunities

Active packaging is a concept in food packaging designed to meet evolving consumer demands and market trends. This approach involves techniques that address various factors, including the absorption of oxygen, ethylene, moisture, carbon dioxide, flavors, and odors and the release of carbon dioxide, antimicrobial agents, antioxidants, flavors, and so much more [8]. This type of packaging is an innovative approach where packaging, product, and environment interact to extend shelf life, enhance safety, or improve sensory properties while preserving product quality. It's especially crucial for fresh and extended shelf-life foods [9].

2.2.2 Active packaging applications

Active packaging materials have a lot of different applications, some of which are relevant to this research.

2.2.2.1 Oxygen scavenging systems

Oxygen is one of the main factors limiting packaged food's shelf life. This is because oxygen will react with the packaged food leading to undesirable chemical changes. For example, oxygen can cause organoleptic changes, accelerate the growth of aerobic bacteria, etc. Oxygen scavenging systems are designed to eliminate oxygen that has permeated through packaging materials into the package during storage and remove any residual oxygen trapped inside the package before it is sealed. These systems are crucial for preserving the quality and extending the shelf life of packaged foods by preventing oxidation [10].

2.2.2.2 Moisture-absorbing and controlling systems.

Excess moisture in food packaging, especially with high-water activity foods like fresh produce and raw meat, can compromise food quality and package integrity. Therefore, food packages commonly include moisture absorbers, primarily through physical adsorption. The absorption capacity is crucial for maintaining product quality [11].

2.2.2.3 Carbon dioxide emitters

Carbon dioxide (CO_2) emitters in packaging extend food shelf life by preventing harmful bacterial growth. They maintain high CO_2 levels to stay effective. However, too much CO_2 can change the food's taste and cause packaging to shrink due to a vacuum effect. CO_2 emitters are often used with oxygen absorbers to keep the packaging intact. These emitters prolong product freshness and make packaging more efficient [12].

2.2.2.4 Ethylene scavengers

Ethylene is a hormone released by the produce, which can accelerate ripening process of various fruits and vegetables. Acceleration in the ripening process can lead to quick maturity and deterioration of food quality, causing changes in taste, odor, color, and potential microbial growth. Therefore, incorporating ethylene scavengers within packaging can mitigate its buildup, extending shelf life and preserving the original food quality. Figure 2 explains the effect of ethylene on fresh fruits.

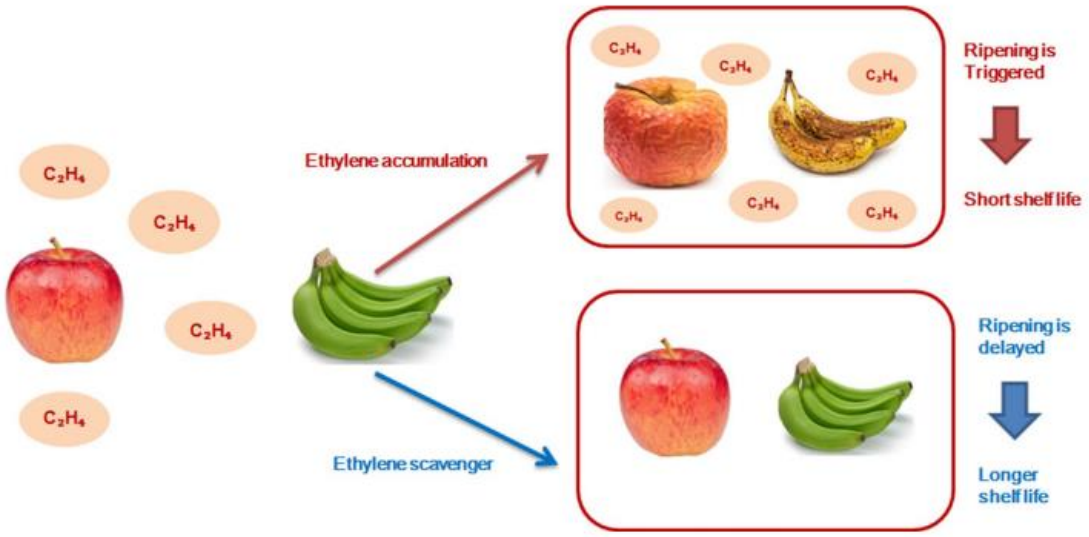

Figure 2: Effect of ethylene accumulation and ethylene scavengers on the shelf life of fruits [13]

Figure 2 shows ethylene accumulation and scavengers' effect on fresh fruits. Here, the ethylene accumulation will decrease the shelf life because it will trigger the fruit ripening. In contrast, ethylene scavengers are used because they will delay the ripening and increase the shelf life [13].

2.2.3 Challenges

Safety and effectiveness of the packaging materials are some of the primary challenges associated with active packaging. Incorporating additives, fillers or active molecular species in the material may impact it is functional properties such as mechanical performance, barrier properties, impacting strength, etc. Additionally, the positive outcomes of antimicrobial packaging can be inconsistent, and affordability remains a significant obstacle, with active packaging potentially doubling end-product costs. Consumer attitudes, favoring products with shorter shelf lives as fresher, also pose obstacles. Moreover, differences in regulatory frameworks between regions, particularly between the US and Europe, further complicate market penetration. Increased collaboration between scientists and industry players could help overcome these obstacles and drive the adoption of next-generation active food packaging technologies. Educating consumers and industry stakeholders about technological advancements will be crucial to foster acceptance and adoption [14].

2.3 Intelligent packaging

2.3.1 Opportunities

Intelligent Packaging (IP) is revolutionizing traditional packaging by integrating advanced communication capabilities. IP encompasses systems capable of detecting, sensing, recording, tracing, and communicating vital information to aid decision-making. This communication functionality is pivotal to extending shelf life, enhancing safety, improving quality, and issuing timely warnings [15].

In the proposed model, as seen in Figure 3, IP assumes a central role as a provider of enhanced communication. Its functionality includes tracking product status, monitoring environmental conditions, and communicating relevant information to consumers or manufacturers, offering early warnings and insights into quality and safety [15].

To simplify the terminology surrounding intelligent packaging, additional terms are avoided. IP represents a system that involves the package, the product, the external environment, and various considerations. Its emergence signifies a paradigm shift, elevating packaging from a passive vessel to an active communicator. By embracing IP, innovative approaches to packaging communication are inspired, enhancing consumer engagement and product safety [15].

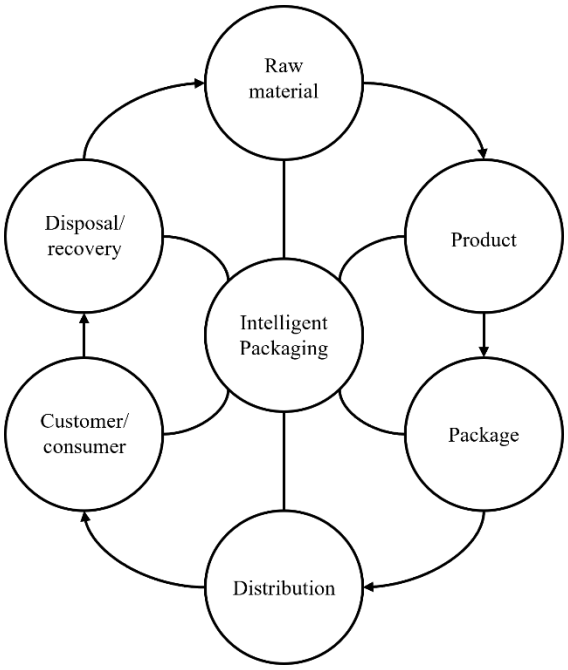

Figure 3: Functions of intelligent packaging in the supply chain [15]

Intelligent packaging can significantly enhance the flow of materials and information within the food supply chain cycle. In Figure 3, the outer circles depict the supply chain cycle, from raw material acquisition through manufacturing, packaging, distribution, product use, and disposal. Traditionally, the package, in varied forms such as pouch, container, drum, or pallet, facilitates material flow (indicated by the arrows in the figure) by containing and protecting the product.

2.3.2 Applications

2.3.2.1 Sensors

A sensor is designed to detect, locate, or measure energy or matter, providing a signal for detecting or measuring a physical or chemical property. Typically, sensors consist of two components: the sensor part, also known as the receptor, which detects the presence, activity, composition, or concentration of specific chemical or physical analytes. The receptor then converts this information into energy that the transducer, the second component, can measure. The transducer converts the measured signal into a proper analytic signal, which may be electrical, chemical, optical, or thermal.

Various sensors exist to investigate different parameters, such as gas sensors, which monitor the concentration of gases like CO_2 or H_2S to determine spoilage progression. CO_2 sensors, for instance, can be non-dispersive infrared or chemical sensors, while O_2 detection may utilize infrared, electrochemical, ultrasonic, or laser technologies. On the other hand, biosensors employ biological materials such as enzymes, antigens, hormones, or nucleic acids in their receptors. These sensors may use electrochemical, optical, acoustic, or other transducers to detect specific pathogens or biochemical compounds and provide visual signals for analysis [16].

2.3.2.2 Indicators

Indicators play a vital role in monitoring the quality and safety of food products throughout the supply chain. They detect the presence or absence of specific substances, the extent of reactions between different substances, or the concentration of particular substances. Time Temperature Indicators (TTIs) are crucial for monitoring temperature fluctuations, which can impact food products' shelf life and safety. Three types of TTIs exist: critical temperature indicators, partial history indicators, and complete history indicators, each serving different functions along the supply chain. These indicators operate based on mechanical, chemical, electrochemical, enzymatic, or microbiological changes in response to time and temperature. Their simplicity makes TTIs user-friendly and user-ready. Freshness indicators track microbiological growth, metabolites, or chemical changes in food products to assess their freshness. Gas indicators monitor changes in the atmosphere inside packaging, detecting variations in oxygen, carbon dioxide, water vapor, and other spoilage-related gases. Advances in technology aim to improve the accuracy and reliability of these indicators, ensuring food safety and quality throughout the supply chain [16].

2.3.3 Challenges

Regulation poses a significant challenge in using chemical substances that may come into contact with food. This area is complex, and legislators are conservative in upholding food safety and consumer health. Presently, the European Union lacks specific regulations concerning dyes as additive permitted for food contact. However, some aspects are addressed in the broader legal framework of active and intelligent packaging intended to come into contact with food (EU No 450/2009) [17]. Without EU directives, guidance from national or regional entities, reference organizations, or associations must be followed.

Key European regulations include EU No 10/2011 on plastics, which outlines positive substances and migration limits, and EU No 1935/2004 on materials intended for contact with food. Additionally, Directive 94/36/EC provides guidelines on colors permitted in food, including positive substances for use in indicators or smart sensors. Therefore, substances in intelligent packaging must be on positive lists. If not, the application system (e.g., diverse coatings) must ensure no contact or migration of substances beyond set limits. Furthermore, these substances must not alter the flavor or appearance of the food [18]. Key USA regulations about active and intelligent packaging are summarized by the U.S. Environmental Protection Agency (EPA) [19].

2.4 Porous materials

2.4.1 Definition and classification

Porous materials have been valued since ancient times, exemplified by the historical use of porous charcoal for medicinal purposes. Porosity is defined as the fraction of pore volume to the total volume of the material [20]. Today, with a renewed global focus on environmental protection and energy conservation, interest in these materials has surged. Their applications span catalysis, separation processes, insulation, sensors, and chromatography, underlining their multidisciplinary significance. The allure of porous structures lies in their capacity to host states of matter inaccessible to homogeneous bulk materials, driving innovation across various fields. However, the efficacy of porous materials heavily depends on their internal pore structure, including geometry, size distribution, connectivity, and surface properties. Thus, comprehensive characterization is essential for optimizing their performance and understanding their behavior in diverse applications. In essence, porous materials are pivotal in modern science and engineering, offering solutions to pressing challenges in environmental sustainability, energy efficiency, and beyond. Their versatility and unique properties drive advancements across numerous disciplines [21].

Pores can also be categorized based on their accessibility to the surroundings, as shown in Figure 4. Pores that connect with the external surface are termed open pores, such as (b), (c), (d), (e), and (f), allowing molecules or ions in the surroundings to enter. Some may only be open at one end, labeled as blind pores (e.g., (b) and (f)), while others are open at both ends, known as through pores (e.g., (e)). Inadequate heating of porous solids may cause parts near the pores' outer shell to collapse, resulting in closed pores (e.g., (a)) that lack communication with the surroundings. Although not involved in adsorption and molecular permeability, closed pores impact solid materials' mechanical properties.

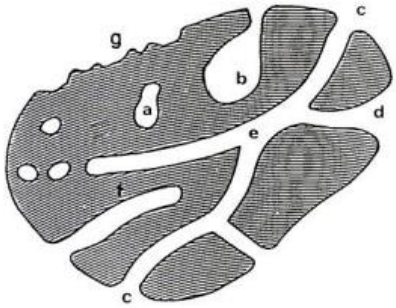

Figure 4: Different types of pores [21]

Within the literature, diverse categories of pore sizes have been delineated. Table 1 summarizes the most commonly employed pore size classifications by the International Union of Pure and Applied Chemistry (IUPAC). However, achieving a consistent classification remains challenging primarily due to discrepancies in delineating macro-, meso--, and micropores, which remains subject of ongoing and vigorous debate.

Table 1: IUPAC Specified types of pores, d [nm] [21]

Classification	Macro-	Meso-	Micro-	Supermicro-	Ultramicro-	Submicro-
IUPAC	> 50	20 < width < 50	< 2	2 < width < 0.7	< 0.7	< 0.4

The IUPAC classification system categorizes pores into macro-, meso-, and micropores, primarily based on the distinct mechanisms observed during N_2 isothermal adsorption at 77 K and 1 atm pressure. The mesopores and micropores correspond to multilayer adsorption, capillary condensation, and micropore-filling processes. Pore widths are classified by applying the capillary condensation theory, which relies on different relative pressures (P/PO ratio). A pore width of 50 nm corresponds to a relative pressure of 0.96. Beyond this threshold, interpreting adsorption isotherm experiments becomes considerably challenging, and the applicability of the capillary condensation theory needs to be examined more.

2.4.2 Types

2.4.2.1 Active carbon

Activated carbon (AC) is prized for its versatility as an adsorbent, boasting a large specific surface area (600–1400 $m^2\ g^{-1}$), well-developed pore structure (0.5–1.4 $cm^3\ g^{-1}$), and high adsorption capacity for volatile organic compounds (VOCs) (10–600 $mg\ g^{-1}$). Derived from various carbonaceous materials such as coal, wood, and coconut shells, AC finds widespread use in environmental applications like wastewater treatment, soil remediation, and air purification. Factors like temperature, concentration, and the presence of specific functional groups influence its effectiveness in adsorbing VOCs. However, challenges remain in its large-scale industrial application due to heel formation during regeneration, flammability, and pore blocking [22].

2.4.2.2 Zeolites

Zeolite is a crystalline aluminosilicate with a three-dimensional arrangement of TO4 tetrahedra (where T is Al or Si), creating channels and cavities for accommodating small organic molecules. Widely used as a chemical sieve, adsorbent, and catalyst, zeolite offers properties such as hydrophobicity, large surface area (250-800 $m^2\ g^{-1}$), and tunable porosities through Si/Al ratio variations. Its superior stability over carbon-based materials, with a lower desorption temperature (150 °C vs. 300 °C), makes it attractive for volatile organic compound (VOC) adsorption. Various zeolite types, including MFI (ZSM-5), FAU (NaX and NaY), beta, SSZ-23, and chabazite, show potential as adsorbents for VOCs. Studies indicate their high adsorption capacities and potential for regeneration, making them comparable to activated carbon. However, the complex and time-consuming synthesis process and the higher cost of source materials present challenges for widespread adoption. Zeolite remains a conventional adsorbent for VOCs due to its high capacity, thermal stability, and reproducibility [22].

2.4.2.3 Metal organic frameworks

MOF, pioneered by Hoskins and Robson (1989), represents a novel class of crystalline hybrid porous materials, constructed from metal ions or clusters coordinated with organic ligands in ordered frameworks. MOFs exhibit outstanding properties such as ultra-high surface area (up to 10000 $m^2\ g^{-1}$), excellent thermal stability and tailorable pore structure [23], [24]. Their open metal sites enhance VOC adsorption capacity, surpassing conventional adsorbents like activated carbon and zeolites. Challenges include high preparation costs and limitations in industrial applications due to weak dispersive forces and insufficient open metal sites. Despite drawbacks, MOFs remain the most promising adsorbent for VOCs due to their tunable pore structure and exceptional properties. Further research is needed to address limitations and fully exploit MOFs' potential in VOC adsorption [22].

2.5 Metal organic frameworks for use in active and intelligent packaging concepts

2.5.1 Introduction

Incorporating these porous MOFs, structures into packaging materials, may offer shelf life extension solution while preserving the nutritional quality of the product [25]. MOFs are innovative porous supramolecular structures that have emerged as a solution to reduce post-harvest food losses and minimize environmental impact [26]. With high surface area and microporosity, MOFs offer tunability, catalytic behavior, and selective adsorption properties. They can be integrated into food packaging materials to extend shelf life by releasing 1-methylcyclopropene (1-MCP), absorbing moisture, absorbing/ releasing oxygen, and detecting microbial contaminants shown in Figure 5. Additionally, MOF-based sensors enable real-time monitoring of food quality parameters, facilitating timely interventions to prevent spoilage and reduce waste. MOFs are solid crystals formed by coordinate bonds between inorganic nodes (like metal ions) and organic linkers. They are well known for their high versability and tunability [27]. Carbonyl-based functions (ex. Imide), oxygen-based functions (ex. Ether), sulfur-based functions (ex. Sulfide), and nitrogen-based functions (ex. Pyridine) are all examples of potential organic linkers Zn^{2+}, Cu^{2+}, Co^{2+}, Ni^{2+} are some of the most used metal ions in MOF structures [28].

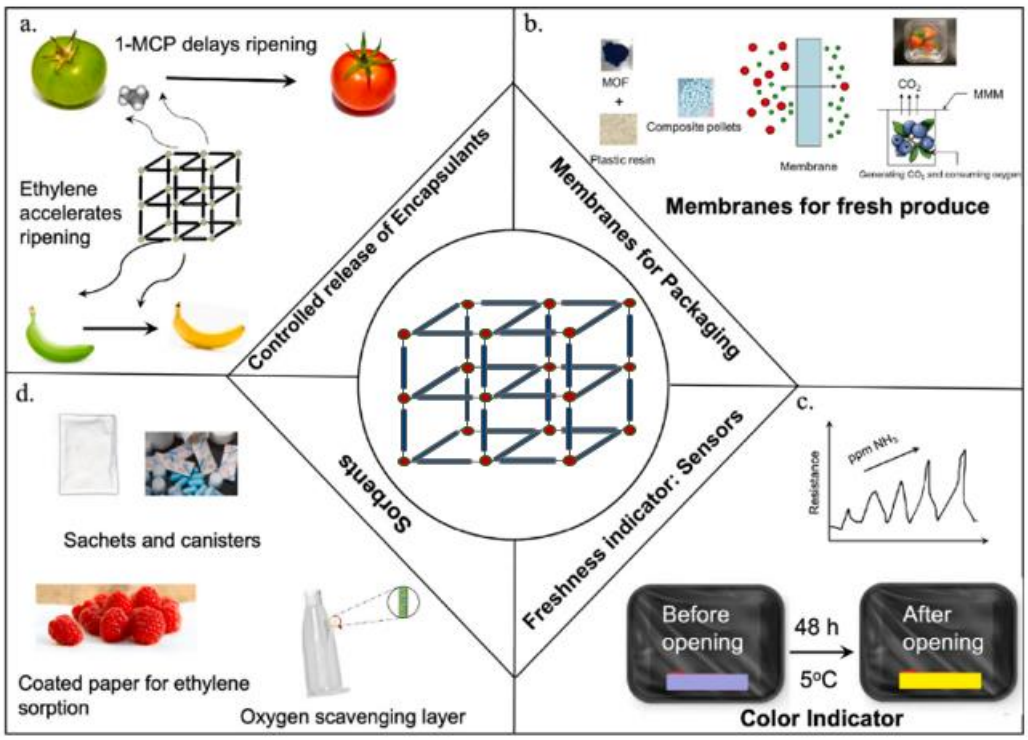

Figure 5: Four potential applications of MOFs: a) release of an encapsulated active component for a controlled shelf life of the product; b) specific permeability characteristics; c) sensors to inform about the freshness of the product; d) absorption of gasses [1]

The potential applications seen in Figure 5 are only a few of the possibilities in the domain of MOFs. More research is needed to optimize the different available MOFs further. Despite their promising potential, challenges such as cost-effectiveness, regulatory approval, and consumer acceptance must be addressed for widespread adoption in the food industry. MOFs consist of two main components: Metal ions and organic linkers, as schematically presented in Figure 1. Reaction between the two, leads to crystal growth and formation of the extended crystal structures. Figure 6 shows an example of a complex microporous 3D structure formed due to the co-ordination of cyclodextrin linker with potassium ions.

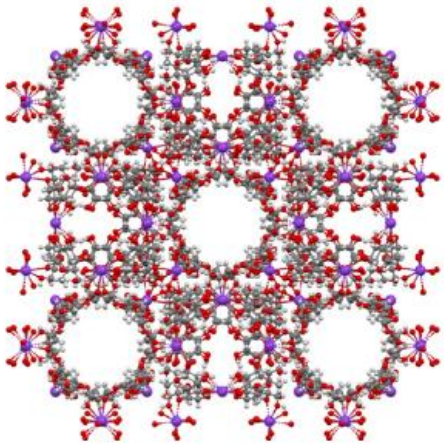

Figure 6: γ-cyclodextrin based MOF (Carbon gray, Oxygen red, Potassium purple) [1]

These MOFs, a novel class of materials, have attracted considerable attention in various industrial sectors, including food-related applications. Over 100,000 MOF structures have been synthesized, with an additional 500,000 theoretically determined. However, most of these structures rely on transition metal ions such as Zn^{2+}, Cu^{2+}, Co^{2+}, and Ni^{2+} and petroleum-derived ligands such as squaramide and urea, which raises concerns about their cytotoxicity and sustainability [28]. Despite these challenges, MOFs hold promise for addressing food additives, flavor enhancement, food packaging, and food sensing issues.

Further research is needed to develop MOFs with safer and more sustainable compositions for broader application in the food industry [29]. In Figure 6: γ-cyclodextrin based MOF (Carbon gray, Oxygen red, Potassium purple) [1]Figure 6, a complex 3D structure can be found with gaps between the networks. These gaps are used to absorb specific gases that can extend the shelf life of the packaged foods or monitor the condition within the packaging.

2.5.2 Types of metal organic frameworks

Metal–organic frameworks (MOFs) can be divided into flexible and rigid types, distinguished by their response to external stimuli: flexible MOFs undergo reversible structural changes, while rigid MOFs maintain their structure. Synthesis-based categorization includes first-generation MOFs with basic structures, second-generation MOFs with surface modifications, and third-generation MOFs incorporating biomolecules. A crystal structure separates crystalline MOFs with regular frameworks from amorphous MOFs with disordered structures. MOFs are classified based on stimulus-response into single-stimuli and multi-stimuli types, providing a comprehensive framework for understanding their diverse properties and applications [25].

2.5.3 Synthesis

Figure 7 shows, seven different methods by which MOFs are synthesized.

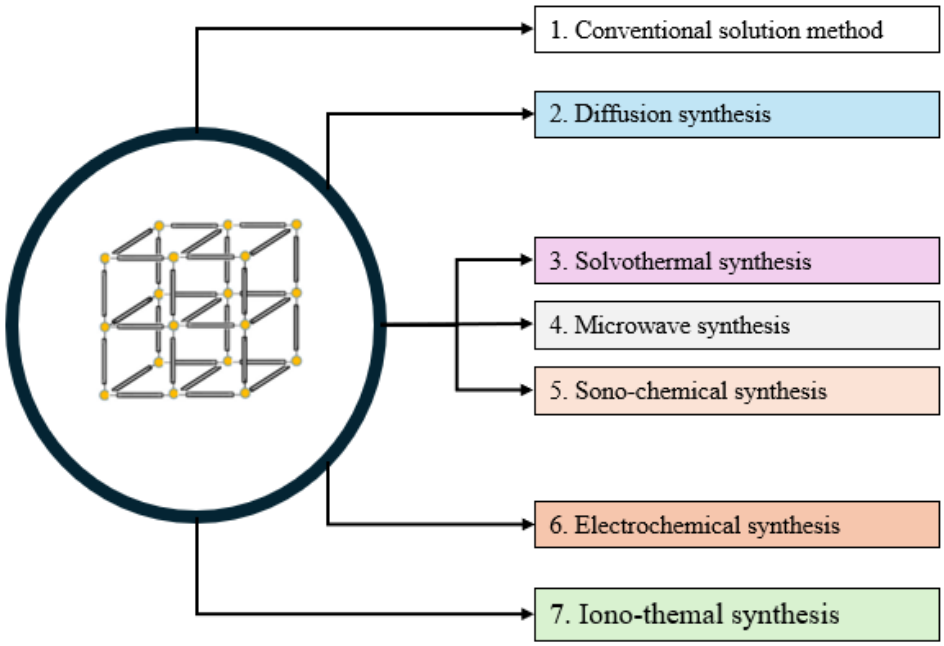

Figure 7: Possible synthesis methods for MOFs

First, in the conventional solution method, organic ligands, metal elements, and other raw materials are mixed in a solvent and stirred at a fixed temperature. The mixture is filtered to separate the reaction products, and solvent evaporation yields MOF crystals. Control over crystal size, symmetry, and calcination temperature is crucial, and it's also used for forming optical ceramics.

Second, the Diffusion Method encompasses the liquid phase diffusion, gel diffusion, and gas-phase diffusion techniques. Liquid phase diffusion involves using an incompatible solvent for organic ligands and metal ions, forming MOF crystals. Gel diffusion mixes metal ions solution with gel substance dispersed with organic ligands, while gas-phase diffusion utilizes a volatile organic ligands solution for MOFs generation. Despite prolonged synthesis times, it's suitable for synthesizing sensitive MOFs under mild conditions.

Solvothermal Synthesis, also known as hydrothermal synthesis when water is used, involves continuously mixing organic ligands, metal ions, and a reaction solvent under set temperature conditions. After the reaction, the mixture is purified to obtain pure MOF crystals. It's an effective method for controlled synthesis with precise temperature regulation.

Microwave-assisted synthesis utilizes microwave radiation to accelerate synthesis by enhancing the interaction between molecules in the solid or liquid mixture. This method is cost-effective, energy-efficient, and provides better control over reaction conditions than traditional heating methods.

Sono-chemical Synthesis employs ultrasound as a heat source to induce rapid heating and cooling rates, leading to accelerated nucleation and reduced crystallization time. This technique produces fine crystallites due to the high-pressure and temperature conditions generated by acoustic cavitation.

Electrochemical Synthesis achieves continuous MOFs synthesis by immersing an anode, a battery cell, and cathode plates in an electrochemical medium. Metal ions are consistently produced due to anodic dissolution, producing higher solid content than batch processes.

Ionic Liquid Medium Synthesis utilizes ionic liquids to substitute organic solvents or conventional water. This technique offers unique properties such as recyclability, zero vapor pressure, and high thermal stability, making it suitable for synthesizing MOFs with specific characteristics [30].

Water-based MOF synthesis offers a sustainable alternative to traditional methods, utilizing water as a non-toxic, stable solvent. It eliminates the need for hazardous organic solvents, leading to environmentally friendly synthesis processes. Super-critical liquids, particularly super-critical CO_2, have emerged as promising solvents for MOF synthesis due to their low toxicity, recyclability, and ease of use [31]. An excellent example of an environmentally friendly synthesis process is mechanochemical synthesis, where a mechanical movement is used to start a chemical reaction between the metal ions and organic linkers. In [5] grinding, a mechanical movement, which starts the reaction between the metal ions and organic linkers, is used to form MOFs.

2.6 Calcium Metal organic frameworks

2.6.1 Advantages

Ca-MOFs are a unique subclass known for their stability, low toxicity, and relatively low density. While less extensively researched than transition metal-based MOFs, Ca-MOFs hold promise for applications in molecular separations, electronics, magnetism, and biomedicine [2]. Their advantages include high biocompatibility for drug delivery and efficient adsorption and storage of light molecules due to their gravimetric benefits. Ca-MOFs, characterized by ionic-like solid bonds due to calcium's high electropositivity, have high thermal stability. With calcium being both highly available and non-toxic, Ca-MOFs are environmentally safe, making them ideal for all applications. Overall, Ca-MOFs present a promising avenue for diverse applications, combining thermal stability, environmental friendliness, gravitational benefits, and cost efficiency [2], [3].

2.6.2 Synthesis

The synthesis of sequential Ca-MOFs involves preparing separate solutions of calcium nitrate tetrahydrate and selected carboxylic linkers in Milli-Q water and N,N-Dimethylformamide (DMF), respectively. These solutions are combined and stirred until effervescence occurs. Subsequently, the mixture undergoes microwave heating at 180°C for 1 hour. After synthesis, the product is collected, washed with DMF to remove the unreacted linker, dried at 70°C, and stored in an airtight desiccator for further analysis [32]. In [33], the adaption of the synthesizes method of Ca-MOFs (Ca-MIX) from existing literature can be found. For the preparation of Ca-MOFs in [34], calcium carbonate and 1,4-benzene-dicarboxylate (in a 1:1 molar ratio) are dissolved in deionized water and DMF, respectively, and then sealed using Teflon. Next, the sample remained in an oven at 110°C for 48 hours. DMF serves as a surfactant to facilitate crystal growth. Following this, filtration is conducted to remove excess solvent, and the mixture is dried in an oven at 110°C for 7 hours. Before use, the sample is dried in a vacuum oven at 110°C for 3 hours. The process is further explained in Figure 8.

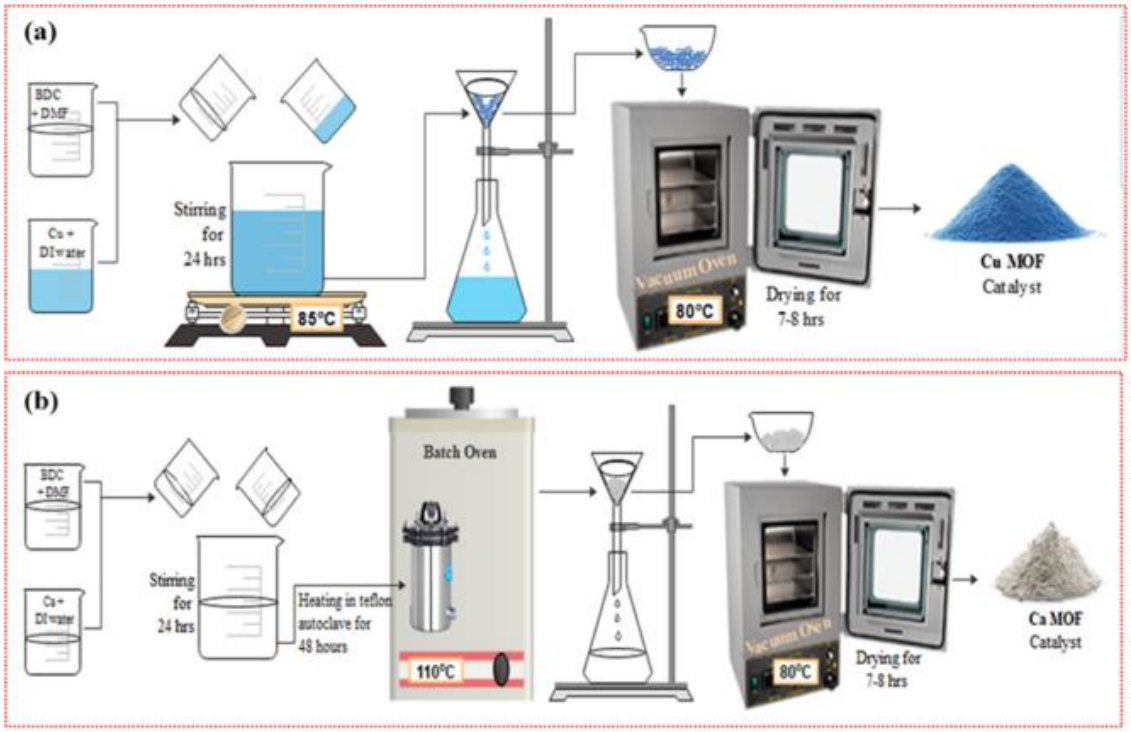

Figure 8: Synthesis of calcium-based MOFs [34]

2.6.3 Mechanochemical synthesis of UTSA-280

Mechanochemical synthesis is a promising synthesis technique for UTSA-280 MOFs where mechanical force, such as grinding, can be used. Grinding initiates chemical reactions between solid reactants and stands out as an up-and-coming method for producing solid materials, particularly MOFs, on a large scale. Its appeal lies in its efficiency for scaling up production and its environmentally friendly characteristics, notably synthesis without harmful solvents. In contrast, traditional methods for synthesizing MOFs are often solvent-heavy and yield low quantities of desired products, with significant by-products complicating industrial applications. Achieving a high atom economy and minimizing waste while maximizing raw chemical conversion efficiency is a considerable challenge in MOF synthesis. The long synthesis time of three days is explained by the slow crystal growth, which takes three days.

While mechanochemical methods typically involve metal salts, such as metal nitrites or chlorides, resulting in additional purification steps due to by-products, using metal oxides or hydroxides offers a promising avenue. Despite the challenge posed by the low solubility of metal oxides/hydroxides, this approach presents a cleaner route, with water being the sole by-product.

In a notable success story, $Ca(C_4O_4)\cdot H_2O$, known as UTSA-280, an ultra-microporous metal-organic framework, was successfully synthesized using mechanochemical methods employing calcium oxide (CaO) or calcium hydroxide ($Ca(OH)_2$). This achievement underscores mechanochemical synthesis's economic and eco-friendly potential for large-scale MOF production. The synthesis process involves grinding a solid mixture of CaO, squaric acid (Figure 9), and water in a mortar for approximately two minutes, forming a light grey powder [5].

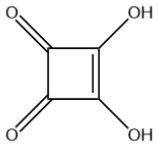

Figure 9: Molecular structure of squaric acid

2.7 Encapsulation of hexanal in metal organic frameworks

2.7.1 Opportunities

Figure 10 shows the molecular structure of hexanal. Hexanal is a promising solution for addressing enzyme activity, ethylene biosynthesis, and other processes contributing to fruit spoilage, browning, and degradation post-harvest.

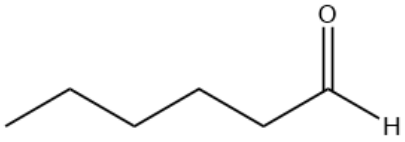

Figure 10: Molecular structure of hexanal

Recent research underscores its effectiveness as a pre-harvest spray, notably prolonging the shelf life of various fruits such as mangoes, strawberries, apples, and more. Hexanal treatment is recognized for enhancing fruit quality without adverse effects; it minimizes browning and spoilage and extends shelf life during storage. Notably, in mangoes, it improves shelf life and fruit quality by fortifying cell membrane integrity. Furthermore, hexanal effectively inhibits the activity of enzymes responsible for fruit deterioration while augmenting antioxidant enzymes and enhancing storage capabilities [35].

2.7.2 Challenges

Hexanal is generally recognized as safe (GRAS) and, therefore, is very interesting because of its antifungal working mechanism. Consequently, it only has one disadvantage: it is very volatile. In other words, it will evaporate fast so that it will escape too fast and will only extend the shelf life by a limited amount [36].

2.7.3 Hexanal encapsulation

In another study, hexanal, was combined with cyclodextrin-based MOFs (CD-MOFs) crystals in equal parts for encapsulation. Ethanol was employed as the solvent to dissolve the hydrophobic hexanal. The hexanal and CD-MOF mixture was stirred in ethanol for an extended period. Cyclodextrin-based MOFs can trap hydrophobic molecules within their structures, allowing for the efficient encapsulation of hexanal. This encapsulation process is facilitated by weak forces such as van der Waals forces, hydrogen bonds, and hydrophobic interactions [37].

2.7.4 Hexanal release

To test the release of hexanal, non-woven fabric sachets were crafted to house hexanal-loaded CD-MOF crystals, each sachet measuring 5 cm × 4 cm and containing 100 mg of crystals. These were sealed and placed in acrylic chambers maintained at 25°C. Hourly sampling from seven chambers over 7 hours enabled the assessment of hexanal release. CD-MOF pellets were dissolved in absolute ethanol, and optical density at 310 nm was measured using a UV−Vis spectrophotometer. A standard graph using hexanal solutions of various concentrations facilitated the determination of release patterns. After each hour, an analysis of the remaining concentrations allowed for precise calculation of hexanal release amounts [37].

2.8 Conclusion

Food waste presents a critical environmental and economic challenge, intensified by greenhouse gas emissions and climate change. Addressing this issue requires innovative solutions in food processing, packaging, and supply chain management. Active packaging technologies play a vital role in extending food shelf life by controlling factors such as oxygen, moisture, and ethylene, which contribute to food spoilage. Despite the promising applications of active packaging, challenges related to safety, cost, and regulatory compliance need to be addressed to enhance market adoption.

Intelligent packaging further revolutionizes the food industry by incorporating advanced sensors and indicators that monitor and communicate the quality and safety of food products. These systems enable real-time tracking and timely interventions, reducing food waste and ensuring consumer safety. However, regulatory hurdles and the complexity of integrating these technologies into existing supply chains remain significant obstacles.

Porous materials, particularly MOFs, offer substantial potential for active and intelligent packaging. its high surface area, tunability, and selective adsorption properties can significantly extend food shelf life and monitor quality. The development of Ca-MOFs, in particular, shows promise due to their biocompatibility, thermal stability, and environmental friendliness. Nevertheless, cost-effective synthesis and regulatory approval are crucial for their widespread application.

In conclusion, integrating advanced packaging technologies, like MOFs, holds promise for mitigating food waste and enhancing the sustainability of food systems. Continued research, collaboration between scientists and industry stakeholders, and addressing regulatory and consumer acceptance challenges are essential for realizing the full potential of these innovative solutions.

3 Materials and Methods

3.1 Materials

3,4-dihydroxy-3-cyclobutene-1,2-dione (squaric acid, 99%) in powder form and hexanal were purchased from Sigma-Aldrich (Milwaukee, WI, USA). CaO was purchased from Himedia (Maharastra, India). Ultra-pure water was purchased from Hanna Instrument (Woonsocket, USA). Hexanal was acquired from consolidated chemicals and solvents (Allentown, PA, USA). Lastly, the A.I. tool ChatGPT was used. The current version of the IEEE style guide does not contain guidelines on this, so this is a facultative agreement [38].

3.2 Synthesis of Calcium based squaric acid metal organic frameworks UTSA-280

The preparation and characterization of UTSA-280 can be divided into three parts: (i) crystal synthesis, (ii) crystal activation, and (iii) crystal analysis.

The first step involved the synthesis and growth of UTSA-280 crystals. The synthesis follows the procedure in Shi et al [5], where squaric acid, CaO, and ultra-pure water were ground using a mortar and pestle for two minutes. The second step is activating the crystals after the synthesis process is completed. This activation is needed to empty the pores since they need to be empty to encapsulate hexanal. Using a similar method found in [39], excess water was removed from the pores using a vacuum oven. The last step was to analyze the activated crystals. Here, XRD and SEM were used to characterize the activated crystals. Lastly, FTIR, DSC, and TGA were used to determine if hexanal was successfully encapsulated.

3.2.1 Crystal synthesis

First, 1.12 g (20 mmol) of CaO was weighed in an aluminum tray. Following, 2.281 g (20 mmol) of squaric acid was weighed in a second aluminum tray. Next, CaO and squaric acid were transferred into the mortar, after which, using a pipet, 1.8 ml of ultra-pure water was added, as seen in Figure 11. After, the mixture was ground for two minutes to complete the reaction. Then, the mixture was transferred to a 15 ml plastic pipe and covered with parafilm to prevent further contamination.

Following synthesis, the crystals need to be washed using deionized water. Washing is essential to separate the unreacted CaO and squaric acid from the reacted UTSA-280 MOFs. CaO and squaric acid have a lower density than UTSA-280 MOFs, so they will float on the water, while UTSA-280 will stay at the bottom. To start the washing step, put half of the synthesized MOFs into a 50 ml beaker. Then, using the squirt bottle, fill the beaker halfway. In the next step, employ a glass stirrer to blend the mixture for a duration of 30 seconds. Subsequently, allow a two-minute interval for the powder to settle at the base. Following this, meticulously transfer the water into a 500 ml beaker, taking care to avoid any powder residue. Repeat these procedures thrice. Finally, facilitate the drying process by leaving the sample undisturbed for 8 hours at 50°C. This last step was executed to prevent water damage in the vacuum oven.

3.2.2 Crystal activation

After synthesis, the crystals need to be activated. Activating UTSA-280 MOFs consists of emptying the pores to prepare the encapsulation process. Therefore, a vacuum oven evaporates excess molecules still in the pores. The sample was placed in the oven, and the temperature was kept constant for 12 hours at 110°C. Lastly, the pressure in the oven was released, and the sample was immediately put in a 15 ml tube to prevent contamination of the pores.

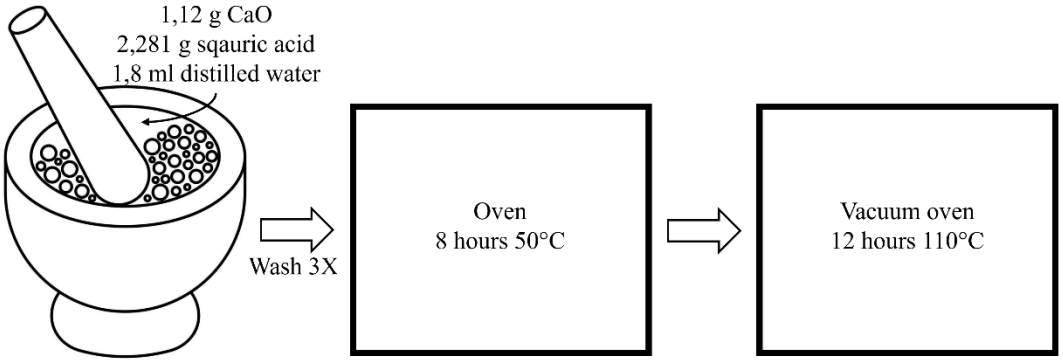

Figure 11: Synthesis and activation of UTSA-280 MOFs

3.3 Hexanal encapsulation

After successfully activating UTSA-280 MOFs, the encapsulation of hexanal was performed. First, 1 g of activated UTSA-280 was transferred into a 50 ml beaker. Next, the beaker was transferred into a 16 oz jar, and 5 ml of hexanal was added to the jar, but not directly into the beaker. After, the metal lid was closed to prevent contamination. Lastly, the encapsulation process was performed for 48 hours. The process is shown in Figure 12.

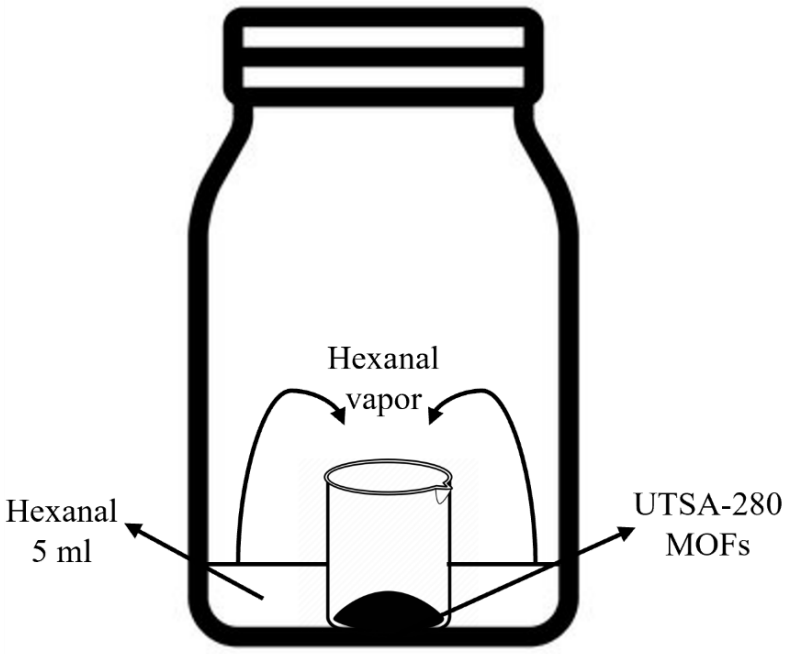

Figure 12: Encapsulation process of hexanal

3.4 Characterization of UTSA-280 MOFs before and after encapsulation

A thorough characterization needs to be performed to investigate the properties and molecular structure of UTSA-280 MOFs before and after encapsulation of hexanal. Different techniques can be used to analyze the MOFs; this study focuses on X-ray diffraction, scanning electron microscopy, thermogravimetric analysis, differential scanning calorimetry, and Fourier transform infrared spectroscopy.

First, XRD was used to determine the crystal structure and chemical composition of the UTSA-280 MOFs. SEM was also performed to confirm the XRD findings and further investigate the MOFs' microstructure. After confirming that the crystals were successfully formed, FTIR, DSC, and TGA were performed. FTIR and TGA were used to verify that the reaction occurred during grinding. Lastly, DSC and TGA were used to investigate whether the hexanal was successfully encapsulated, with TGA determining the amount of hexanal encapsulated.

3.5 X-Ray diffraction

XRD is a non-destructive technique used to determine the structure of mostly solid materials. Therefore, this method can identify amorphous or crystalline structures within solid samples. It can also analyze material properties like phase composition, structure, and texture. This is done by comparing the XRD patterns of reference samples. Therefore, it can be compared to determining a fingerprint since it is different for every material. Due to the regular arrangement of atoms in solid materials, the X-rays will be scattered, leading to constructive interference at specific angles. To describe the diffraction and interference of X-rays in a crystal, Bragg's law (formula 1) defines it as a reflection at the atomic planes of the crystal lattice [40].

$$2d\sin(\theta) = n\lambda \qquad (1)$$

Where:

- d = interplane spacing
- θ = Bragg angle (2θ = angle between incident and reflected beam)
- n = order of interference
- λ = wavelength

The intensity of a reflection is determined by the structure factor (symmetry of the crystal, position of the atoms, number of electrons of the atoms), the amount of material and the absorption in the material [40].

Figure 13: RIGAKU X-ray diffraction machine

Rigaku Miniflex Diffractometer (Rigaku, TX, USA), utilizing CuKα radiation (k = 1.5418 Å, k=2π/λ, λ=0.154 nm) at 40 kV and 30 mA, was employed to characterize the activated UTSA-280 and hexanal encapsulated crystals. Data collection involved a nickel filter within the 2 to 40° 2θ range, with increments of 0.02, at a scan speed of 0.9° min^{-1} [41].

3.6 Scanning electron microscopy

The analysis involves electron beam application within a high-energy range (100-30,000 electron volts), typically emitted from a thermal source. SEM lenses compress and focus the electron beam onto the specimen to produce a sharp image, with most SEMs achieving spot sizes less than 10 nm. The image formation occurs point by point as the electron beam is directed by scan coils, creating a raster pattern on the specimen's surface. The electron detector collects emitted signals essential for image generation, including secondary electrons (S.E.) and backscattered electrons (BSE). Control of brightness and intensity is crucial for image clarity, with magnification beyond 10,000x necessary for detailed examination. The electron voltage mode affects image details, with low voltages providing surface information and higher voltages penetrating deeper into the sample. The resulting SEM image reveals topographic features such as shape, size, and surface texture, influenced by the number of collected S.E. and BSE signals. Increasing the sample's tilt angle enhances topographic contrast by elevating signal numbers [42], [43]. These measurements were necessary to investigate the microstructure compared to just the atomic structure; using these results, the XRD graphs could also be confirmed.

Figure 14: JEOL-7800F SEM

SEM was conducted using the JEOL-7800F setup (JEOL Ltd., Tokyo, Japan) at an acceleration voltage of 15 kV under a high vacuum. These tests were done both on the activated UTSA-280 MOFs and the UTSA-280 MOFs after encapsulation of hexanal. Since MOFs are not conductive, a gold coating was applied to obtain images successfully.

3.7 Thermogravimetric analysis

TGA is a technique used to analyze materials by monitoring their mass as they are subjected to controlled temperature changes in a controlled environment. Essentially, it measures how the weight of a sample changes as it is heated or cooled in a furnace. This method provides valuable insights into the material's thermal stability, decomposition, and other temperature-dependent properties [44].

Figure 15: TA Q50 TGA machine

TGA was conducted using a TA Q50 TGA machine (T.A. Instruments, New Castle, DE). The analysis was conducted under a nitrogen atmosphere, with a balance purge flow rate set at 40 ml min^{-1} and a sample purge flow rate of 60 ml min^{-1}. Samples weighing approximately 5-10 mg were loaded into platinum pans for analysis. The samples were tested at a heating ram rate of 10°C min^{-1}, starting from room temperature to 700°C. These controlled conditions allowed for the investigation of the specimen's thermal properties and decomposition behavior.

3.8 Differential scanning calorimetry

DSC can detect if any guest molecules, mostly hydrocarbon gasses, are found in the pores. Here, DSC can determine thermal properties, like melting point T_m of the impurities in the UTSA-280 pores. Therefore, this measurement was only executed after the encapsulation of hexanal.

Figure 16: DSC Q1000

Experiments were performed using the DSC Q1000 (T.A. Instruments, New Castle) in the range of 0 to 230°C. A hermetically sealed aluminum crucible weighed the samples (approximately 5 mg per sample). An identical pan was used as a reference. The samples were heated at ten °C/min during constant nitrogen purging of 50 ml/min. Measurements were always performed in triplicate. Lastly, the data was analyzed using Universal Analysis software version 1000 (T.A. Instruments, New Castle).

3.9 Fourier transfer infrared spectroscopy

FTIR is a technique used to measure the absorption and emission spectra in the infrared region. It aims to determine how effectively a sample absorbs light at different wavelengths. Different molecular structures exhibit distinct spectra due to unique vibrational frequencies associated with each type of bond. Analyzing the infrared spectra makes it possible to distinguish between various substances and gather structural information about molecules. Each type of bond, such as N-H, C-H, or O-H, absorbs infrared radiation within specific spectrum regions, allowing for precise identification and characterization [45], [46].

Figure 17: FTIR machine

FTIR spectra were obtained using a weakened total reflectance module FTIR spectrometer (Shimadzu MIRacle 10 Single reflection ATR accessory FTIR, CA). The experiments were conducted in triplicate. Each sample was measured with 45 scans with a resolution of 4 cm^{-1} across a range of 500 cm^{-1} to 4000 cm^{-1}. Infrared measurements were performed at room temperature, with a gain setting of 1 and Square Triangle apodization. Background spectra for reduction were also collected at room temperature.

4 Results and discussion

4.1 Synthesis of UTSA-280 metal organic framework

The synthesis of UTSA-280 MOFs was performed using a mechanochemical synthesis technique. A grey powder was formed after grinding for two minutes, as shown in Figure 18. Prepared samples include UTSA-280 without activation or hexanal encapsulation, UTSA-280 post-activation without encapsulation, and UTSA-280 post-activation with hexanal encapsulation. These were meticulously prepared for comparative analysis to understand the impact of each step on UTSA-280's properties.

Figure 18: UTSA-280 MOF powder

4.2 X-ray diffraction analysis before and after hexanal encapsulation

Figure 19 shows the XRD spectrum obtained after the activation of the formed crystals. These measurements were performed to evaluate the crystal quality before and after encapsulation.

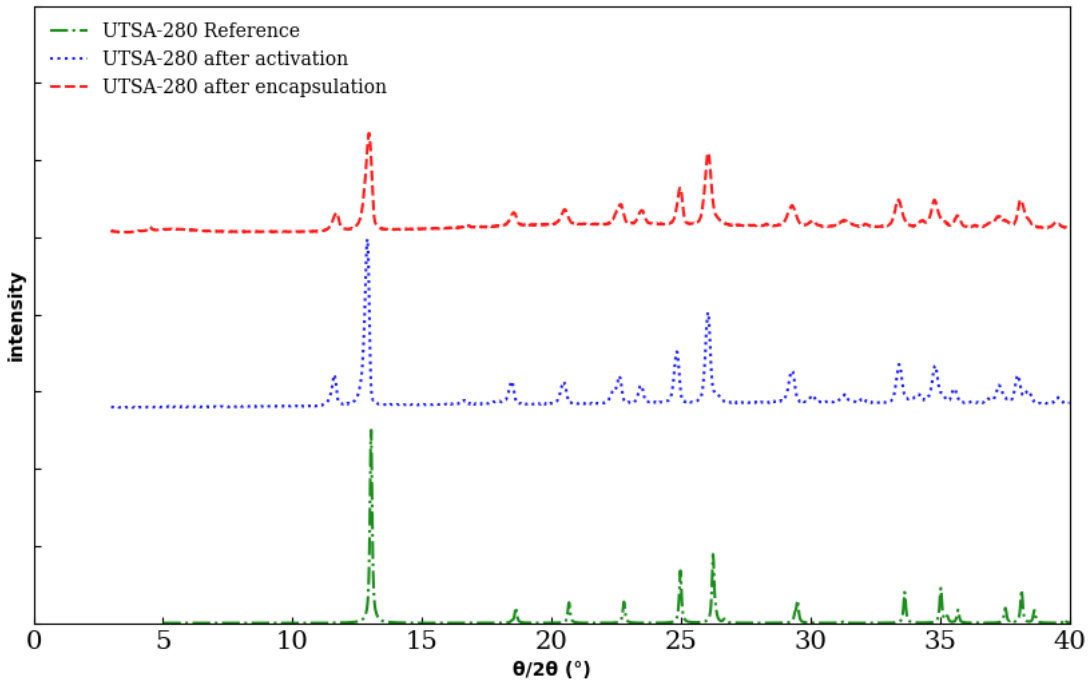

Figure 19: XRD results of UTSA-280 MOFs after activation

Strong XRD diffraction patterns indicate the highly crystalline nature of the synthesized structure. Similar diffraction peaks are observed in the simulated and synthesized structure support successful synthesis of the crystal structure. The crystals maintained their structure after the encapsulation process. Furthermore, when these measurements are compared to the reference data, it is evident that a similar crystal structure has been achieved, with some minor differences around 12° and 24°. This conclusion

is supported by the observation that the ratio of the peaks in the sample closely matches that of the reference, indicating that the crystalline integrity and composition are preserved throughout the procedures.

4.3 Analyzing the UTSA-280 MOF structures using FTIR

To further establish whether the reaction was successful, FTIR spectroscopy was conducted. This analysis was performed on the individual substances and the synthesized UTSA-280 crystals, both before and after activation. In addition, UTSA-280 was measured on FTIR before and after encapsulation of hexanal.

Figure 20 represents the molecular structure of the repeating unit of UTSA-280. Figure 21 contains all obtained FTIR results. Initially, CaO and squaric acid were analyzed, and the resulting spectra were validated against previously reported measurements in the literature [47], [48]

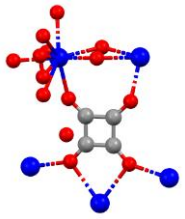

Figure 20: Molecular structure of UTSA-280 (red = oxygen, blue = calcium, grey = carbon)

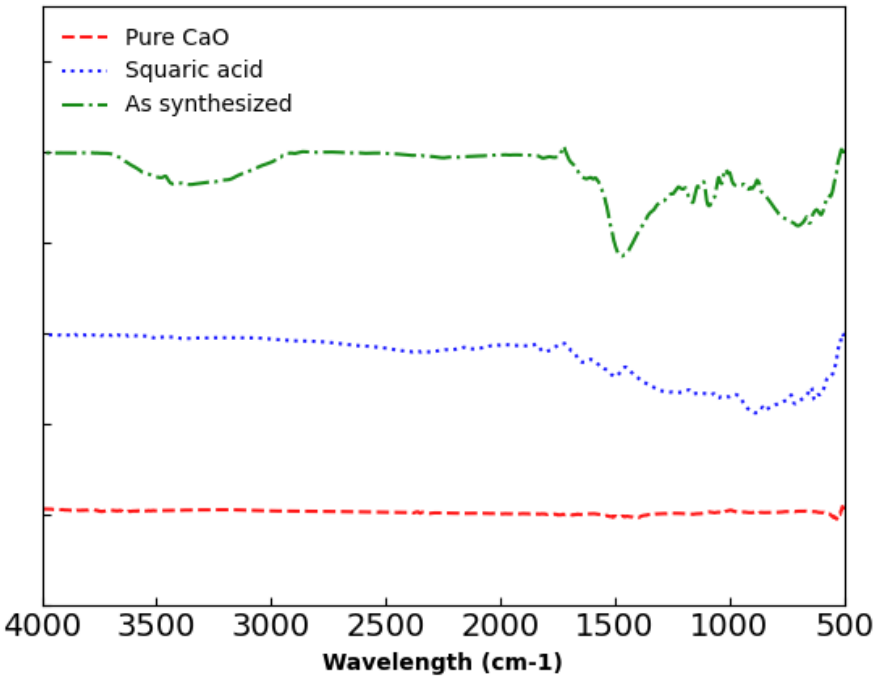

Figure 21: FTIR results of CaO, squaric acid, and UTSA-280 MOFs before activation

In the FTIR spectrum of squaric acid, a small peak at 1804 cm^{-1} is attributed to the asymmetric stretching vibration of the C=O bond. Overlapping vibrations of the C=C and C=O bonds appear around 1500 cm^{-1}. Furthermore, the bands observed at 1292 and 712 cm^{-1} correspond to the C-C stretching vibration and the symmetric motion of the C-C bond within the ring, respectively. Next, the FTIR spectrum of CaO does not display any significant peaks compared to those of squaric acid and the synthesized UTSA-280. Lastly, in the FTIR spectrum of synthesized UTSA-280, a peak between 3500-3300 cm^{-1} is observed due to the O-H bonds.

In addition to analyzing the CaO and squaric acid, FTIR spectroscopy was conducted on UTSA-280 MOFs before and after activation. Additionally, pure hexanal was tested, and the FTIR results, along with those obtained after activation and following the encapsulation of hexanal in UTSA-280, are presented in Figure 22.

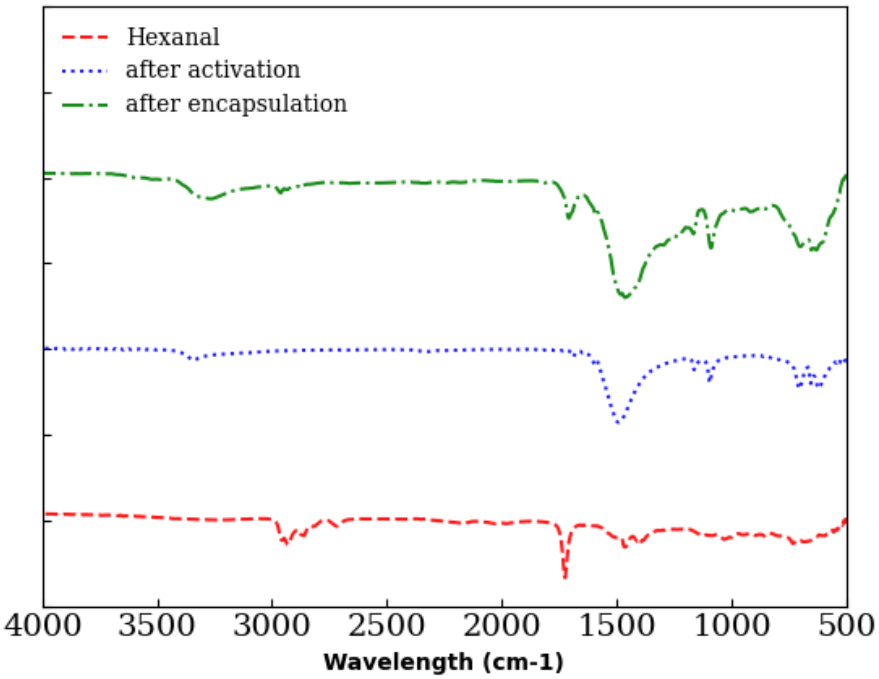

Figure 22: FTIR spectra of hexanal, UTSA-280 MOFs before and after encapsulation

When comparing FTIR curves with earlier findings in the literature, it can be concluded that the reaction between CaO and squaric acid, to form UTSA-280 crystals, was successful during the two-minute grinding process [48], [49]. After activation, it can be seen that the peak due to the O-H bonds becomes much smaller than before activation due to the loss of water during activation. In addition to the smaller O-H peak, a change in the fingerprint area is obtained due to the loss of water and any other molecules that were sucked out of the pores during activation. The FTIR spectra of pure hexanal and UTSA-280 after encapsulation are detailed. Figure 23 zooms in on some specific wavelength regions to distinguish the peaks more.

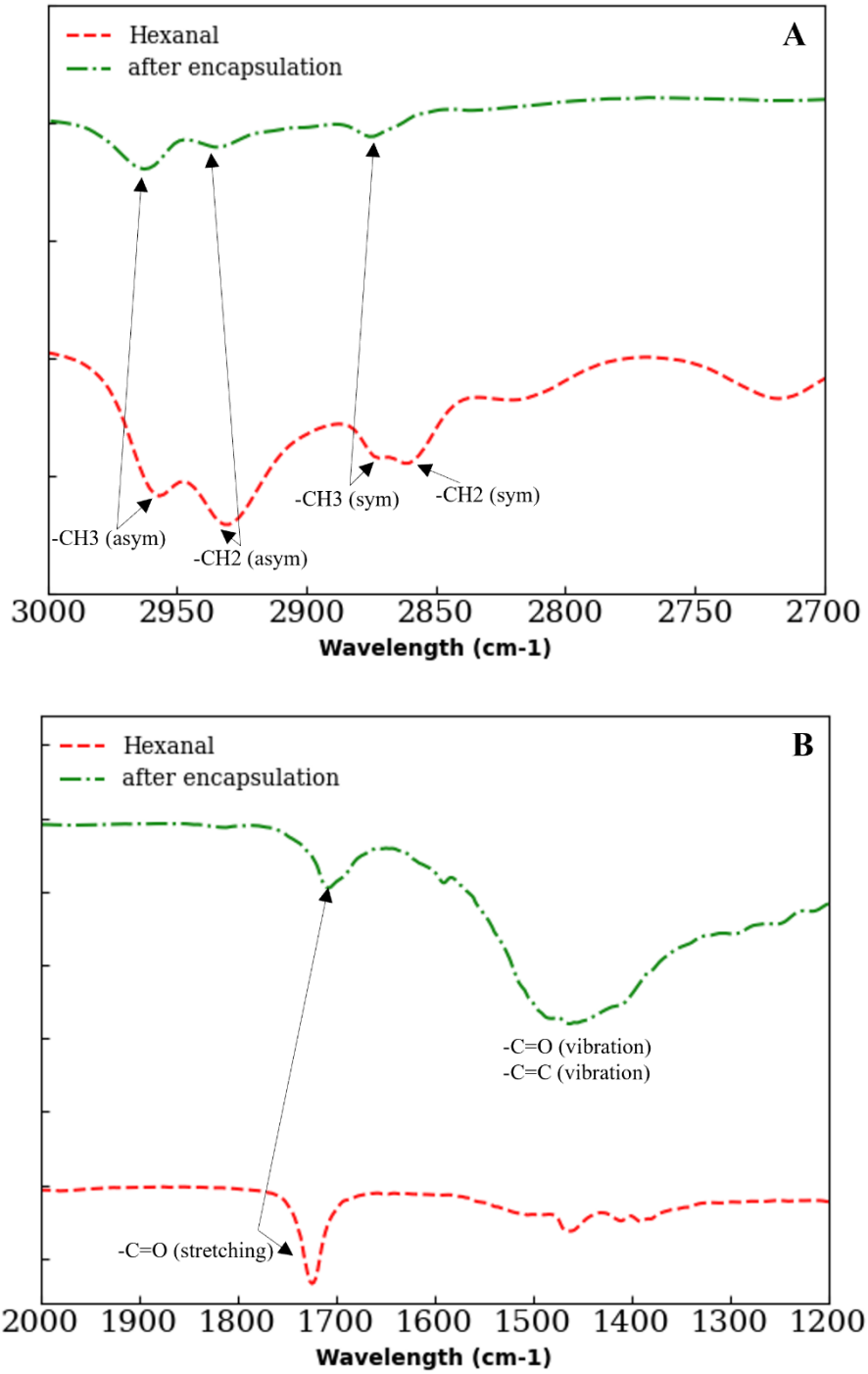

Figure 23: FTIR results of hexanal and UTSA-280 after encapsulation: A) 3000-2700 cm^{-1}, B) 2000-1200 cm^{-1}

After encapsulation, the peak around 3300 cm^{-1} indicates that not all water was removed during activation. A peak at 3000 cm^{-1} and various peaks in Figure 23A are attributed to $-CH_3$ and $-CH_2$ symmetric and asymmetric stretching. Specifically, at 2975 cm^{-1}, $-CH_3$ asymmetric stretching is observed in hexanal and encapsulated samples. Peaks at 2930 cm^{-1} and 2875 cm^{-1} correspond to $-CH_2$ asymmetric stretching and $-CH_3$ symmetric stretching, respectively. A peak at 2850 cm^{-1} is only seen in the hexanal sample due to symmetric $-CH_2$ stretching. Figure 23B shows a peak at 1720 cm^{-1} caused by -C=O bond stretching. Additionally, a significant peak around 1500 cm^{-1} is due to the overlapping vibrations of the C=C and C=O bonds. These observations confirm that the encapsulation of hexanal was successful.

4.4 Thermogravimetric analysis on UTSA-280 MOFs

TGA was performed to analyze the thermal properties of UTSA-280 crystals. In addition, These measurements could give a better insight if the encapsulation process was successful. Figure 24 shows weight loss and derivative weight in function of the temperature for the different samples measured. Initially, a weight loss between 50-95°C was observed, attributed to the loss of H_2O molecules. The weight loss between 150-300°C is explained by H_2O coordinated with Ca^{2+} ions. Any weight loss beyond 392°C is attributed to the decomposition of the UTSA-280 MOFs framework. [50], [51], [52]. The obtained graph after activation aligns with the literature. Therefore, the formed UTSA-280 MOFs are thermally stable compared to previous studies [48]. As expected, no significant change can be found around 100°C after activation because most water was removed during the activation process.

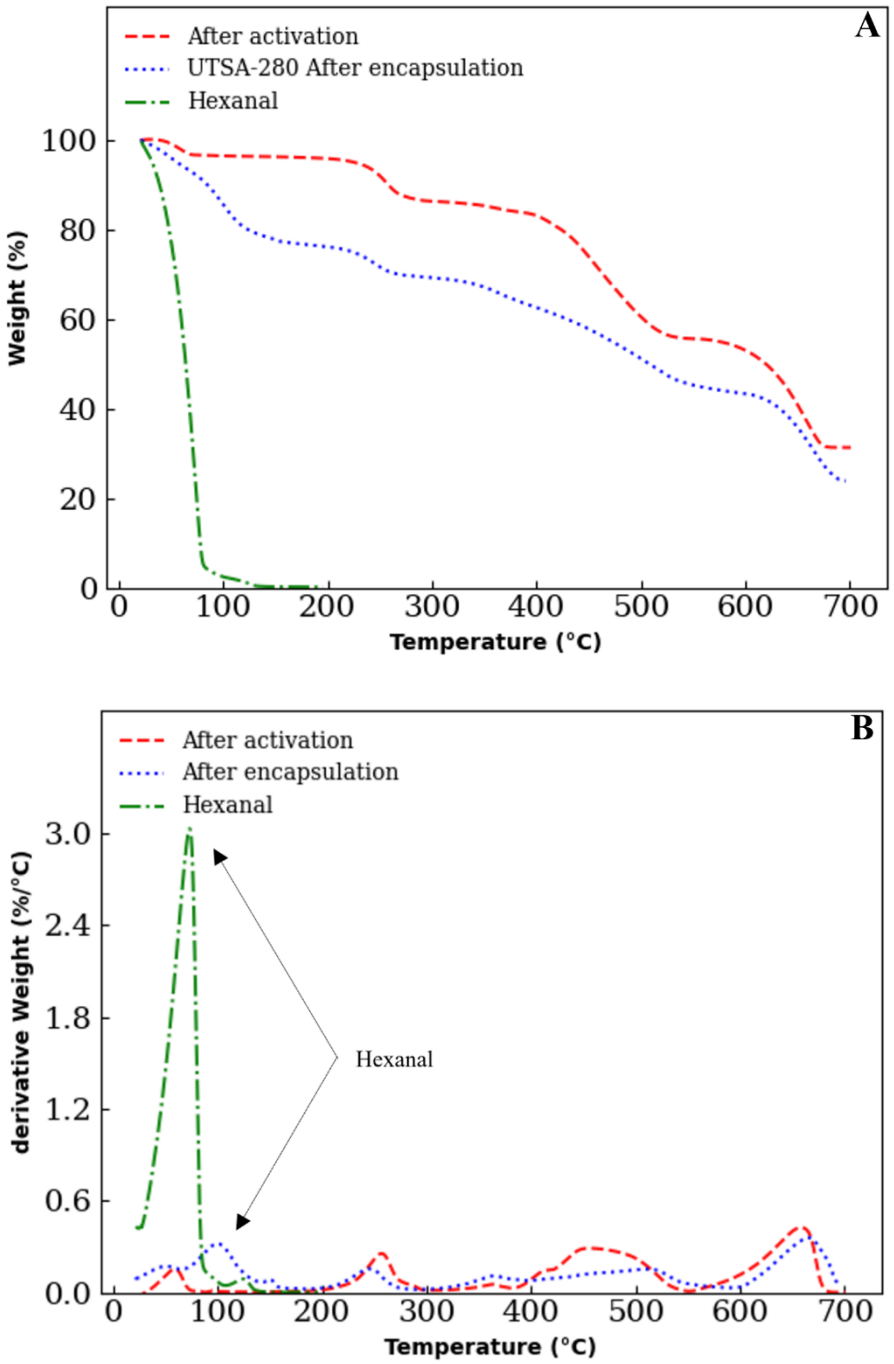

Figure 24: TGA results of pure hexanal and UTSA-280 before and after encapsulated with hexanal: A) weight (%) in function of temperature, B) derivative weight in function of temperature

When comparing the weight loss of pure hexanal, which begins at 70°C, to the first significant weight loss of the encapsulated MOFs, which starts at 100°C, it is evident that hexanal evaporates at a higher temperature when encapsulated. This indicates successful encapsulation of hexanal within the MOF's pores, as hexanal must first be released from the pores before it can evaporate. This explains why hexanal begins to disappear at 70°C before encapsulation but at 100°C after encapsulation, with a slower rate of evaporation post-encapsulation.

Lastly, the amount of hexanal encapsulated in UTSA-280 MOFs must be determined. This was achieved by measuring the weight loss at 200°C for both the sample after activation and encapsulation. The temperature of 200°C was selected because, at this point, all water present in the samples had evaporated, ensuring that any observed weight loss could be linked solely to the loss of hexanal. These calculations are summarized in Figure 25.

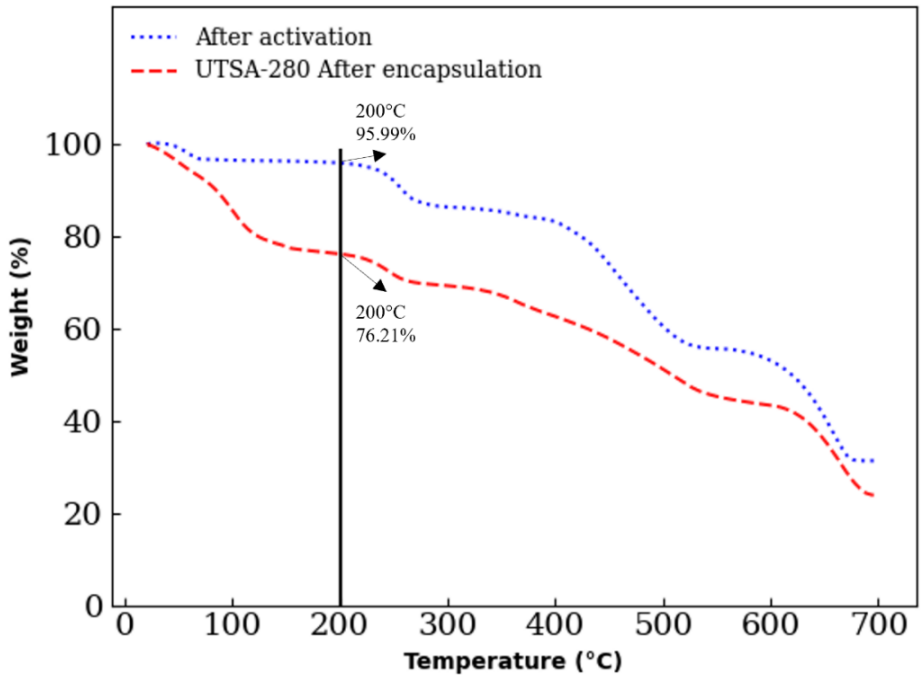

Figure 25: Weight loss at 200°C for UTSA-280 after activation as well as after encapsulation

First, it can be seen that at 200°C, the weight (wt%) after activation is still at 95.99 wt%. This value must be compared with the weight at 200°C after encapsulation, which is 76.21 wt%. The amount of hexanal encapsulated can be determined when calculating the difference between these two values. It can be concluded that a percentage of 19.78 wt% hexanal can be encapsulated in the UTSA-280 MOFs after activation.

4.5 Differential scanning calorimetry on UTSA-280 MOFs

DSC was employed to validate the observations derived from TGA analysis.. Figure 26 contains the different DSC measurements that were performed. First, pure hexanal was measured, followed by UTSA-280 after activation and encapsulation.

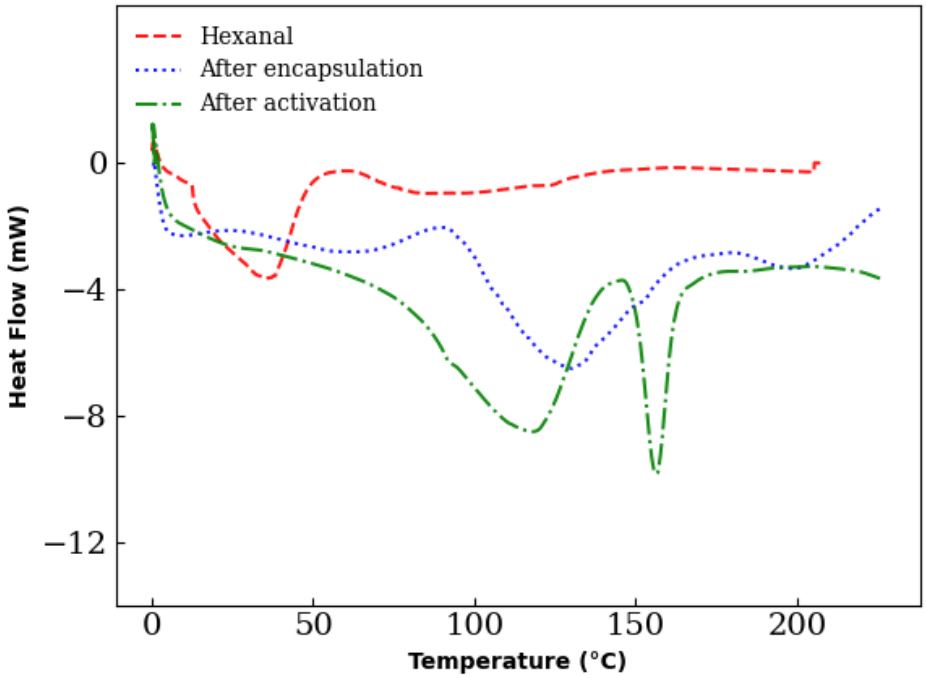

Figure 26: DSC results of pure hexanal and UTSA-280 MOFs before and after encapsulation

A peak at 40°C characterizes the evaporation of pure hexanal. However, after encapsulation, the evaporation peak shifts to 100-150°C and becomes bigger, indicating successful encapsulation. The bigger size of the peak can be explained by the excess water still present in the sample. This significant temperature difference confirms that the hexanal is effectively trapped within the pores of the MOF. Additionally, after encapsulation, a peak is observed at approximately 200°C, which suggests that hexanal is coordinated with Ca^{2+} ions. Following activation, a peak is detected around 120°C, which is due to the water still present after activation. In addition, a peak between 150-170°C is formed, indicating the presence of strong secondary bonding between the different components of MOF, within the encapsulated structure.

4.6 Crystal structure analysis of UTSA-280 MOFs using scanning electron microscopy

Figure 27 shows the SEM images captured after the encapsulation process. Two images were collected on different parts of the sample to confirm that crystals maintained their structure.

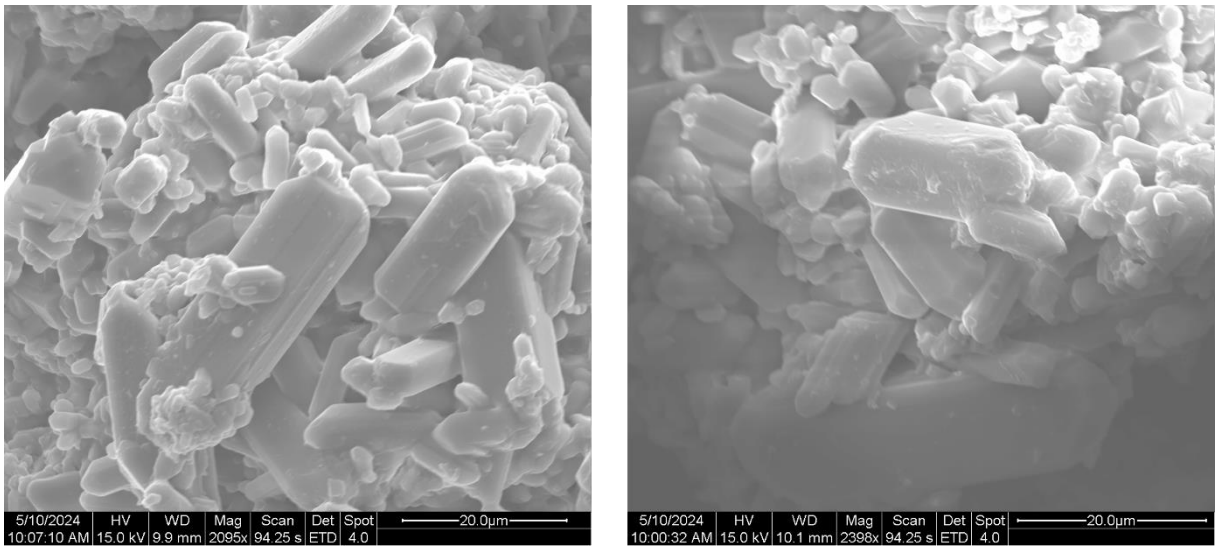

Figure 27: SEM images of UTSA-280 after encapsulation

After analyzing the SEM images of UTSA-280 post-encapsulation, the findings of the XRD analysis can be confirmed. The XRD results indicated that UTSA-280 crystals were successfully synthesized and they retained their structure post encapsulation. This was further validated by the SEM images, where the crystals were visible. This visual confirmation from the SEM underscores the successful formation and integrity of the UTSA-280 crystals after encapsulation. The combined evidence from SEM and XRD analyses ensures the reliability of the encapsulation method.

5 Conclusion

In conclusion, the synthesis of UTSA-280 MOFs through mechanochemical synthesis was achieved, yielding a grey powder. Through XRD analysis conducted before and after hexanal encapsulation, a highly crystalline structure was observed. It was concluded that the crystals stay intact during the encapsulation process as well as that the crystals obtained resemble the reference UTSA-280 crystals. FTIR spectroscopy provided further insight by confirming chemical interactions among the reactants and the formation of the desired MOFs before activation and following hexanal encapsulation.

TGA indicated the thermal stability of UTSA-280 MOFs, showcasing weight losses attributed to the evaporation of encapsulated hexanal. DSC corroborated this, which displayed a shift in the evaporation temperature post-encapsulation, further confirming the successful encapsulation of hexanal within the MOF structure. Lastly, TGA results indicated that 19.78 wt% of hexanal was successfully encapsulated in the UTSA-280 MOFs, demonstrating the method's effectiveness in achieving the desired capacity.

SEM images validate the integrity of UTSA-280 crystals post-encapsulation. In agreement with XRD data, this visual evidence establishes that the UTSA-280 crystals remained intact throughout the encapsulation process.

Together, these comprehensive analyses underscore the reliability and robustness of the synthesized UTSA-280 MOFs, highlighting their potential for various applications in fields such as catalysis, gas storage, and drug delivery. Further research and optimization of synthesis techniques may enhance the efficiency and scalability of UTSA-280 MOF production, opening avenues for broader utilization in industrial and academic settings.

Future work could involve integrating these encapsulated UTSA-280 MOFs into food packaging materials. This innovation holds promise for extending the shelf life of perishable food items, contributing to reduced food waste and enhanced food safety. By leveraging the unique properties of UTSA-280 MOFs, such as their high surface area and tunable pore sizes, it becomes feasible to develop packaging materials that actively absorb and neutralize harmful gases, moisture, and odors, thereby preserving the freshness and quality of packaged foods over extended periods. Furthermore, incorporating encapsulated MOFs into food packaging aligns with the growing demand for sustainable and environmentally friendly solutions. Through continued research and development in this direction, the potential impact on food preservation and waste reduction could be substantial, benefiting both consumers and the environment.

Reference List

[1] A. Kathuria, A. El Badawy, S. Al-Ghamdi, L. S. Hamachi, and M. B. Kivy, "Environmentally benign bioderived, biocompatible, thermally stable MOFs suitable for food contact applications," *Trends in Food Science and Technology*, vol. 138. pp. 323–338, Aug. 01, 2023. doi: 10.1016/j.tifs.2023.06.024.

[2] S. Xian, Y. Lin, H. Wang, and J. Li, "Calcium-Based Metal–Organic Frameworks and Their Potential Applications," *Small*, vol. 17, no. 22. John Wiley and Sons Inc, Jun. 01, 2021. doi: 10.1002/smll.202005165.

[3] R. H. Shi *et al.*, "Two calcium-based metal organic frameworks with long afterglow as anticounterfeiting materials," *Chemical Engineering Journal*, vol. 479, Jan. 2024, doi: 10.1016/j.cej.2023.147851.

[4] L. Carl, "CALCIUM-BASED SQUARIC ACID METAL ORGANIC FRAMEWORKS FOR POST COMBUSTION CARBON CAPTURE," pp. 17-20. Jun. 2023.

[5] Y. Shi, B. Liang, A. Alsalme, R. B. Lin, and B. Chen, "Mechanochemical synthesis of an ethylene sieve UTSA-280," *J Solid State Chem*, vol. 287, Jul. 2020, doi: 10.1016/j.jssc.2020.121321.

[6] A. Sharma, H. K. Bons, S. K. Jawandha, and S. W. Chung, "Hexanal Application Extends Shelf-life and Maintains Quality of 'Umran' Indian Jujube Fruit by Regulating Antioxidant Activities During Cold Storage," *Erwerbs-Obstbau*, 2023, doi: 10.1007/s10341-023-00963-z.

[7] E. Almenar, R. Auras, M. Rubino, and B. Harte, "A new technique to prevent the main post harvest diseases in berries during storage: Inclusion complexes β-cyclodextrin-hexanal," *Int J Food Microbiol*, vol. 118, no. 2, pp. 164–172, Sep. 2007, doi: 10.1016/j.ijfoodmicro.2007.07.002.

[8] L. Vermeiren, F. Devlieghere, M. Van Beest, N. De Kruijf, and J. Debevere, "Developments in the active packaging of foods," pp. 77-86, 1999.

[9] P. Suppakul, J. Miltz, K. Sonneveld, and S. W. Bigger, "Active packaging technologies with an emphasis on antimicrobial packaging and its applications," *Journal of Food Science*, vol. 68, no. 2. Institute of Food Technologists, pp. 408–420, 2003. doi: 10.1111/j.1365-2621.2003.tb05687.x.

[10] Y. Byun, D. Darby, K. Cooksey, P. Dawson, and S. Whiteside, "Development of oxygen scavenging system containing a natural free radical scavenger and a transition metal," *Food Chem*, vol. 124, no. 2, pp. 615–619, Jan. 2011, doi: 10.1016/j.foodchem.2010.06.084.

[11] K. K. Gaikwad, S. Singh, and A. Ajji, "Moisture absorbers for food packaging applications," *Environmental Chemistry Letters*, vol. 17, no. 2. Springer, pp. 609–628, Jun. 15, 2019. doi: 10.1007/s10311-018-0810-z.

[12] S. Haghighi-Manesh and M. H. Azizi, "Active packaging systems with emphasis on its applications in dairy products," *Journal of Food Process Engineering*, vol. 40, no. 5. Blackwell Publishing Inc., Oct. 01, 2017. doi: 10.1111/jfpe.12542.

[13] K. K. Gaikwad, S. Singh, and Y. S. Negi, "Ethylene scavengers for active packaging of fresh food produce," *Environmental Chemistry Letters*, vol. 18, no. 2. Springer, pp. 269–284, Mar. 01, 2020. doi: 10.1007/s10311-019-00938-1.

[14] M. W. Ahmed *et al.*, "A review on active packaging for quality and safety of foods: Current trends, applications, prospects and challenges," *Food Packaging and Shelf Life*, vol. 33. Sep. 01, 2022. doi: 10.1016/j.fpsl.2022.100913.

[15] K. L. Yam, P. T. Takhistov, and J. Miltz, “Intelligent packaging: Concepts and applications,” *Journal of Food Science*, vol. 70, no. 1. Institute of Food Technologists, 2005. doi: 10.1111/j.1365-2621.2005.tb09052.x.

[16] P. Müller and M. Schmid, “Intelligent packaging in the food sector: A brief overview,” *Foods*, vol. 8, no. 1. MDPI Multidisciplinary Digital Publishing Institute, 2019. doi: 10.3390/foods8010016.

[17] P. Suppakul, J. Miltz, K. Sonneveld, and S. W. Bigger, “Active packaging technologies with an emphasis on antimicrobial packaging and its applications,” *Journal of Food Science*, vol. 68, no. 2. Institute of Food Technologists, pp. 408–420, 2003. doi: 10.1111/j.1365-2621.2003.tb05687.x.

[18] E. Poyatos-Racionero, J. V. Ros-Lis, J. L. Vivancos, and R. Martínez-Máñez, “Recent advances on intelligent packaging as tools to reduce food waste,” *J Clean Prod*, vol. 172, pp. 3398–3409, Jan. 2018, doi: 10.1016/j.jclepro.2017.11.075.

[19] K. K. Gaikwad, S. Singh, and A. Ajji, “Moisture absorbers for food packaging applications,” *Environmental Chemistry Letters*, vol. 17, no. 2. Springer, pp. 609–628, Jun. 15, 2019. doi: 10.1007/s10311-018-0810-z.

[20] A. Del and R. R. Cardona, “INVESTIGATION OF ZEOLITE NUCLEATION AND GROWTH USING NMR SPECTROSCOPY A Dissertation,” 2011.

[21] B. D. Zdravkov, J. J. Čermák, M. Šefara, and J. Janků, “Pore classification in the characterization of porous materials: A perspective,” *Central European Journal of Chemistry*, vol. 5, no. 2, pp. 385–395, Jun. 2007, doi: 10.2478/s11532-007-0017-9.

[22] L. Zhu, D. Shen, and K. H. Luo, “A critical review on VOCs adsorption by different porous materials: Species, mechanisms and modification methods,” *Journal of Hazardous Materials*, vol. 389. May 05, 2020. doi: 10.1016/j.jhazmat.2020.122102.

[23] F. Ambroz, T. J. Macdonald, V. Martis, and I. P. Parkin, “Evaluation of the BET theory for the characterization of meso and microporous MOFs,” *Small Methods*, vol. 2, no. 11. John Wiley and Sons Inc, 2018. doi: 10.1002/smtd.201800173.

[24] P. Z. Moghadam *et al.*, “The Development of a CSD Subset: A Collection of Metal-Organic Frameworks for Past, Present and Future,” 2017. [Online]. Available: http://people.ds.cam.ac.uk/df334

[25] A. Sultana, A. Kathuria, and K. K. Gaikwad, “Metal–organic frameworks for active food packaging. A review,” *Environmental Chemistry Letters*, vol. 20, no. 2. Springer Science and Business Media Deutschland GmbH, pp. 1479–1495, Apr. 01, 2022. doi: 10.1007/s10311-022-01387-z.

[26] A. M. Yimer, A. H. Assen, I. El Mghaimimi, O. Lakbita, K. Adil, and Y. Belmabkhout, “Unlocking the potential of phosphogypsum waste: Unified synthesis of functional metal-organic frameworks and zeolite via a sustainable valorization route,” *Chemical Engineering Journal*, vol. 479, Jan. 2024, doi: 10.1016/j.cej.2023.147902.

[27] W. Cheng, X. Tang, Y. Zhang, D. Wu, and W. Yang, “Applications of metal-organic framework (MOF)-based sensors for food safety: Enhancing mechanisms and recent advances,” *Trends in Food Science and Technology*, vol. 112. pp. 268–282, Jun. 01, 2021. doi: 10.1016/j.tifs.2021.04.004.

[28] S. Ali Akbar Razavi and A. Morsali, “Linker functionalized metal-organic frameworks,” *Coordination Chemistry Reviews*, vol. 399. Nov. 15, 2019. doi: 10.1016/j.ccr.2019.213023.

[29] A. Kathuria, T. Harding, R. Auras, and M. B. Kivy, "Encapsulation of hexanal in bio-based cyclodextrin metal organic framework for extended release," *J Incl Phenom Macrocycl Chem*, vol. 101, no. 1–2, pp. 121–130, Oct. 2021, doi: 10.1007/s10847-021-01095-1.

[30] P. S. Sharanyakanth and M. Radhakrishnan, "Synthesis of metal-organic frameworks (MOFs) and its application in food packaging: A critical review," *Trends in Food Science and Technology*, vol. 104. pp. 102–116, Oct. 01, 2020. doi: 10.1016/j.tifs.2020.08.004.

[31] A. Al Obeidli, H. Ben Salah, M. Al Murisi, and R. Sabouni, "Recent advancements in MOFs synthesis and their green applications," *International Journal of Hydrogen Energy*, vol. 47, no. 4. pp. 2561–2593, Jan. 12, 2022. doi: 10.1016/j.ijhydene.2021.10.180.

[32] M. Q. J. Roslan, A. Z. Aris, M. B. A. Rahman, L. H. Ngee, N. M. Isa, and N. F. A. Aljafree, "Mechanistic synthesis of a sequential calcium-carboxylate-based linker (Ca-MOFs) and rapid assessment of chemical stability through XRD analysis," *J Mol Struct*, vol. 1303, May 2024, doi: 10.1016/j.molstruc.2024.137566.

[33] F. F. Sukatis, M. Q. Jori Roslan, L. J. Looi, H. N. Lim, M. B. Abdul Rahman, and A. Z. Aris, "Process variables optimization for synthesizing novel calcium-based metal-organic frameworks for feasible synthetic estrogen adsorption," *Microporous and Mesoporous Materials*, p. 112822, Sep. 2023, doi: 10.1016/j.micromeso.2023.112822.

[34] U. Jamil, A. Husain Khoja, R. Liaquat, S. Raza Naqvi, W. Nor Nadyaini Wan Omar, and N. Aishah Saidina Amin, "Copper and calcium-based metal organic framework (MOF) catalyst for biodiesel production from waste cooking oil: A process optimization study," *Energy Convers Manag*, vol. 215, Jul. 2020, doi: 10.1016/j.enconman.2020.112934.

[35] A. Sharma, H. K. Bons, S. K. Jawandha, and S. W. Chung, "Hexanal Application Extends Shelf-life and Maintains Quality of 'Umran' Indian Jujube Fruit by Regulating Antioxidant Activities During Cold Storage," *Erwerbs-Obstbau*, 2023, doi: 10.1007/s10341-023-00963-z.

[36] E. Almenar, R. Auras, M. Rubino, and B. Harte, "A new technique to prevent the main post harvest diseases in berries during storage: Inclusion complexes β-cyclodextrin-hexanal," *Int J Food Microbiol*, vol. 118, no. 2, pp. 164–172, Sep. 2007, doi: 10.1016/j.ijfoodmicro.2007.07.002.

[37] V. Nagarajan, S. Kizhaeral S, M. Subramanian, S. Rajendran, and J. Ranjan, "Encapsulation of a Volatile Biomolecule (Hexanal) in Cyclodextrin Metal-Organic Frameworks for Slow Release and Its Effect on Preservation of Mangoes," *ACS Food Science and Technology*, vol. 1, no. 10, pp. 1936–1944, Nov. 2021, doi: 10.1021/acsfoodscitech.1c00205.

[38] "OpenAI, "ChatGPT," 4 Oktober 2023 [online]. Available: https://chatgpt.com/.

[39] Y. Gong *et al.*, "Selective Uptake of Ethane/Ethylene Mixtures by UTSA-280 is Driven by Reversibly Coordinated Water Defects," *Chemistry of Materials*, vol. 35, no. 7, pp. 2956–2966, Apr. 2023, doi: 10.1021/acs.chemmater.3c00065.

[40] Martin. Ermrich, Detlef. Opper, and PANalytical (Almelo), *XRD for the analyst : getting acquainted with the principles*. PANalytical, 2013.

[41] A. Kathuria, Y. S. Lee, J. Shin, and M. Kivy, "Crystalline γ-cyclodextrin metal organic framework nano-containers for encapsulation of benzaldehyde and their host–guest interactions," *J Incl Phenom Macrocycl Chem*, vol. 102, no. 9–10, pp. 781–790, Oct. 2022, doi: 10.1007/s10847-022-01158-x.

[42] Azad, M. and Avin, A. Scanning Electron Microscopy (SEM): A Review. Proceedings of 2018 International Conference on Hydraulics and Pneumatics, HERVEX, Baile Govora, Romania, 7-9 November 2018, 1-9.

[43] Zhou, Weilie & Apkarian, Robert & Wang, Zhong & Joy, David. (2006). Fundamentals of Scanning Electron Microscopy (SEM). 10.1007/978-0-387-39620-0_1.

[44] PerkinElmer, "A Beginner's Guide to Thermogravimetric Analysis," 2010.

[45] Verma, Rahul. (2022). Introduction to Fourier Transform Infrared Spectrometry. 10.13140/RG.2.2.21043.71206.

[46] W. Herres and J. Gronholz, "Series Understanding FT·IR Data Processing Part 1: Data Acquisition and Fourier Transformation," 2007.

[47] R. Foroutan, R. Mohammadi, H. Esmaeili, F. Mirzaee Bektashi, and S. Tamjidi, "Transesterification of waste edible oils to biodiesel using calcium oxide@magnesium oxide nanocatalyst," *Waste Management*, vol. 105, pp. 373–383, Mar. 2020, doi: 10.1016/j.wasman.2020.02.032.

[48] X. Chen, G. Chen, G. Liu, G. Liu, and W. Jin, "UTSA-280 metal–organic framework incorporated 6FDA-polyimide mixed-matrix membranes for ethylene/ethane separation," *AIChE Journal*, vol. 68, no. 8, Aug. 2022, doi: 10.1002/aic.17688.

[49] X. L. Xiong, G. H. Chen, S. T. Xiao, Y. G. Ouyang, H. B. Li, and Q. Wang, "New Discovery of Metal-Organic Framework UTSA-280: Ultrahigh Adsorption Selectivity of Krypton over Xenon," *Journal of Physical Chemistry C*, vol. 124, no. 27, pp. 14603–14612, Jul. 2020, doi: 10.1021/acs.jpcc.0c02280.

[50] K. S. Lee, J. J. Kweon, I. H. Oh, and C. E. Lee, "Polymorphic phase transition and thermal stability in squaric acid (H 2C 4O 4)," *Journal of Physics and Chemistry of Solids*, vol. 73, no. 7, pp. 890–895, Jul. 2012, doi: 10.1016/j.jpcs.2012.02.013.

[51] J. Song *et al.*, "Ca2+-based metal-organic framework as enzyme preparation to promote the catalytic activity of amylase," *Mater Today Chem*, vol. 30, Jun. 2023, doi: 10.1016/j.mtchem.2023.101522.

[52] K. G. Sakellariou, G. Karagiannakis, Y. A. Criado, and A. G. Konstandopoulos, "Calcium oxide based materials for thermochemical heat storage in concentrated solar power plants," *Solar Energy*, vol. 122, pp. 215–230, Dec. 2015, doi: 10.1016/j.solener.2015.08.011.